SERI/TR-8104-4-T3
(DE81026049)

LOW-COST PROCESS FOR P-N JUNCTION-TYPE SOLAR CELL

Final Report for the Period September 1, 1980—February 28, 1981

By
John B. Mooney
Robert H. Lamoreaux
Clayton W. Bates, Jr.

February 1981

Work Performed Under Contract No. AC02-77CH00178

SRI International
Menlo Park, California

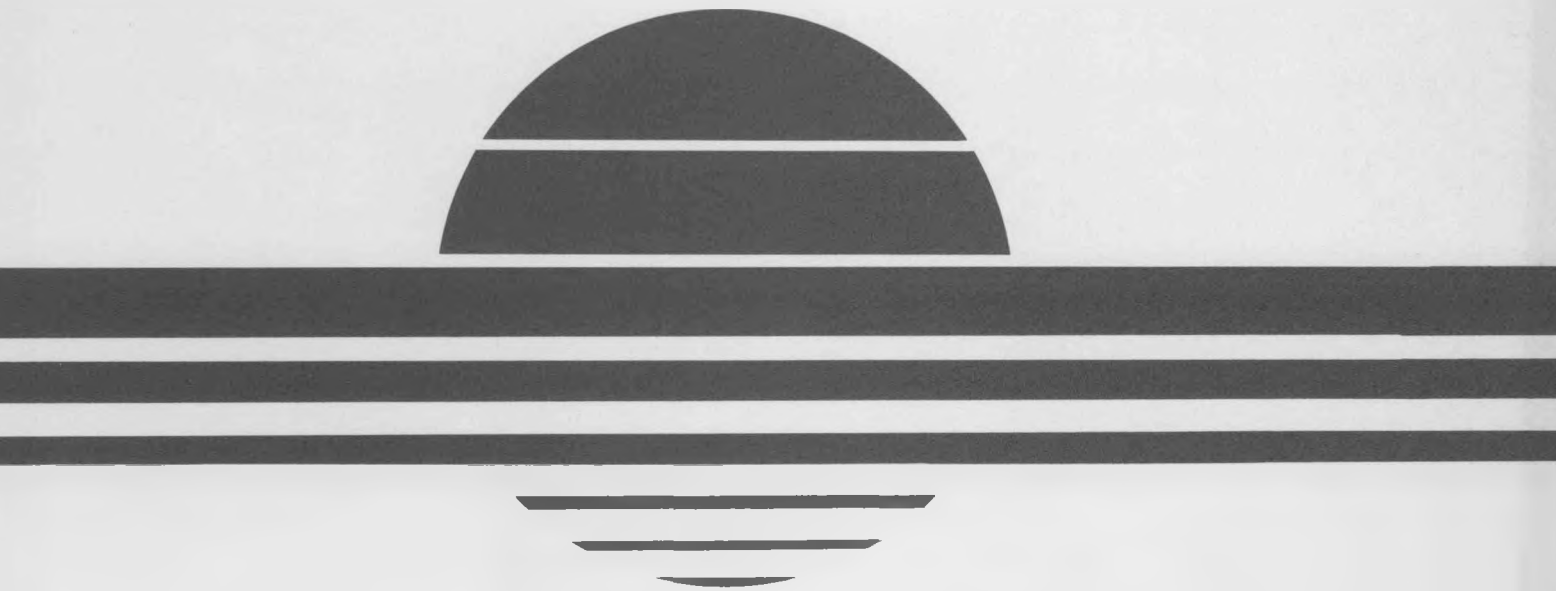

U.S. Department of Energy

Solar Energy

SERI/TR-8104-4-T3
(DE81026049)
Distribution Category UC-63

LOW-COST PROCESS FOR P-N JUNCTION-TYPE SOLAR CELL

Final Report

Covering the Period 1 September 1980 to 28 February 1981

February 1981

By: John B. Mooney, Senior Research Chemist
Engineering Sciences Laboratory

Robert H. Lamoreaux, Visiting Chemist
Materials Research Laboratory

Clayton W. Bates, Jr., Professor
Stanford University

Prepared for:

Solar Energy Research Institute
Photovoltaics Program Office
1536 Cole Boulevard
Golden, Colorado

Attn: Leon Fabick

SERI Subcontract XS-9-8104-4 under EG-77-C-01-4042

SRI Project 8833

Approved:

Fred J. Kamphoefner, Director
Engineering Sciences Laboratory

Earle D. Jones, Vice President
Advanced Development Division

Blank Page

ILLUSTRATIONS

factor, and consequent low efficiency. The major problems appear to be in CdS film density and in junction deliniation.

CONTENTS

ABSTRACT

We have studied low-cost manufacturing methods for two types of thin-film solar cells on glass substrates. One is a heterojunction CdS/$CuInSe_2$ deposited by chemical spray pyrolysis; the other is a CdS/CdTe cell that is prepared by silk screening and sintering.

In the spray pyrolysis program, we have succeeded in deposition CdS layers that, after a brief heat treatment in nitrogen-cadmium atmosphere, have a resistivity of less than 0.1 Ω-cm. We have also spray-deposited $CuInSe_2$ films that after a brief heat-treatment exhibit the desired chalcopyrite structure. Heterojunctions with photovoltaic response were produced by spray pyrolysis. The fill factors were low; consequently, the efficiency was less than 1 percent. The conditions for heat-treatment of the two layers of the heterojunction are mutually incompatible, and the resistance of the CdS layer increases during the $CuInSe_2$ deposition. Also, the condition for the conversion of the sphalerite to chalcopyrite seems to destroy the junction.

A chemical thermodynamiic study of the spray pyrolysis process has been useful in understanding and directing the spray pyrolysis program.

Future work will be directed toward configurations and techniques that will produce chalcopyrite $CuInSe_2$ and low-resistivity CdS.

The sintered cells are prepared by first applying a CdS layer containing a $CdCl_2$ flux and $GaCl_2$ dopant to a borosilicate glass substrate. The layer is sintered in a nitrogen-cadmium atmosphere, then a CdTe layer (also containing $CdCl_2$ flux) is applied and sintered in nitrogen. The CdTe is converted to p-type by immersion in a CuCl solution. Metalic paint electrodes are then applied. We have obtained photovoltaic response with V_{oc} ranging up to 0.6 V, but with low I_{sc} and fill

TABLES

CONCISE DESCRIPTION OF THE PROJECT

The objectives of this project are to fabricate nonsilicon thin film solar cells of two types on glass substrates:

- A heterojunction CdS/$CuInS_2$ (and $CuInSe_2$) deposited by chemical spray pyrolysis.
- A solar cell based on silk screened and sintered CdTe.

This program entails four tasks

(1) Spray pyrolyze ITO (indium tin oxide) CdS, $CuInS_2$, and $CuInSe_2$ with properties necessary for solar cell applications. Determine optimum conditions.

(2) Prepare chlorine-doped CeTe powders, prepare films of these powders on ITO and CdS surfaces by screen printing and sintering, determine optimum conditions, and conduct a thermodynamic and kinetic study of the printing and sintering process.

(3) Develop photovoltaic devices with a goal of 8 percent efficiency and at least 1 cm^2 area.

- Glass/Au/p-$CuInS_2$/CdS/Al
- Glass/Au/p-$CuInSe_2$/CdS/Al
- Glass/Au/p-cu$InSe_2$/$Cd_{0.84}Zn_{0.16}A$/Al
- Glass/ITO/CdS/n-CdTe/p-CdTe/Cu_2Te or graphite/Au
- Glass/ITO/Cds/n-CdTe/p-CdTe/Cu_2S/Au
- Optimize and apply antireflective coatings.

(4) Evaluate the layers and devices, to characterize and optimize the materials and devices, including cell stability and degradation mechanisms. Stanford University (Prof. C.W. Bates, Jr.) is a subcontractor in this task.

I INTRODUCTION AND SUMMARY

This program began on 1 September 1979 with two major objectives:

- Prepare a solar cell using spray pyrolysis to deposit of all but the contact metalization, and having the structure glass/Au grid/p-$CuInSe_2$/n-CdS/Al.
- Prepare screen-printed and sintered solar cells of the composition glass/IT/CdS/n-CdTe/p-CdTe/p-Cu_2Te/Au.

The significant results of the spray-pyrolysis program are:

- By spray pyrolysis from a solution deficient in thiourea, we have produced a CdS film that has a post-heat-treatment resistivity of less than 0.1 Ω-cm.
- Films of $Cd_{0.84}Zn_{0.16}S$ with 1 Ω-cm resistivity have been produced.
- Stoichiometric films of $CuInS_2$ have been prepared from a solution with a Cu:In:S = 2:1:10 concentration ratio.
- Thermodynamic calculations with a free-energy minimization program have predicted a different ideal composition for $CuInSe_2$.
- Stoichiometric films of $CuInSe_2$ have been prepared from a solution with a Cu:In:Se = 1:1:4. As predicted, more selenium led to a second phase of $Cu_{2-x}Se$.
- A chalcopyrite layer has been produced with a small excess of copper at Cu:In:Se of 1.1:1:4 and a 600°C, 5-minute heat treatment.
- A heterojunction glass/IT/CdS/$CuInS_2$ exhibited the photovoltaic effect.
- A heterojunction of CdS/$CuInSe_2$ in both the front-wall and back-wall configuration exhibited the photovoltaic effect.
- The best devices to date had 0.2 V_{oc} and 12 A/cm^2 I_{sc}, but with less than 30 percent full factor and less than 1 percent efficiency.
- A $Cd_{0.84}Zn_{0.16}S$/$CuInSe_2$ back-wall cell had a 0.24 V_{oc} and 7.2 A/cm^2 I_{sc}.

Future work will be directed toward device analysis with the results guiding the process development. We will concentrate on the back-wall configuration.

The screen-printed and sintered cell development is more of a literature study to understand the devices that have been reported, and repeat this work. To date, we have

- Produced coherent CdS films of about 1 Ω-cm resistivity and 50 percent density.
- Produced photovoltaic devices with a 0.41 V_{oc} and a 0.74 A/cm^2 I_{sc}. The fill factor is less than 30 percent and efficiency is low.
- The best results to date have been without the transparent conductor.

Future work will be directed toward improved density and the definition and control of the junction.

II STUDIES OF SPRAY PYROLYSIS

A. Apparatus

We have used three different apparatus for the spray pyrolysis experiments. All have been designed to spray areas of up to 3 x 4 inches in a nitrogen atmosphere. The spray was in constant motion to eliminate irregularities that might result from imperfections in the spray gun. The glass (Corning 7059 substrate glass), which is a borosilicate glass of approximately 750 μm thickness, is floated on a liquid metal bath (Cd-free Pb/Sn solder). In the first two systems, the tin bath was translated perpendicularly to the heaters in a 2-inch reciprocating motion of 6 cycles per minute. The spray head was a Spraying Systems 1/4 J head with spray setup No. 11. The heat is supplied by a pair of 1-kW quartz lamps arranged in a direction parallel to the motion of the head. The inert atmosphere is maintained by the nitrogen spraying gas passing through narrow openings around the bottom of the chamber. The first two systems containing the translating substrate heater were found to have two major difficulties of contamination with oxygen from an imperfect seal around the base (partially related to the requirement of substrate motion) and iron contamination resulting from attack of the acidic solutions from the CuInSe. The iron contamination was eliminated by using Pyrex spraying nozzle. This nozzle was tested in a chamber which did not incorporate motion of the spray head or the substrate. The resultant films were not as uniform as those obtained with the earlier system; however, the CuInSe, contained less oxygen. Because oxygen contamination is a serious problem, we have modified the system that does not include substrate motion to incorporate a circular motion of the spray head. The new system has a uniform spray distribution over an area up to 2 x 2 inches and does not include translation or motion of the substrate. The seal to the base is much superior and the back diffusion of oxygen is largely eliminated. Preliminary CdS films were

sprayed in air; these films were uniform, but contained a relatively high pinhole density. Films that were produced in the spray chambers not only had less oxygen contamination, but had fewer pinholes.

The surface temperature during spraying is a critical experimental variable. The published data on temperature effects have all been related to the temperature of a heater (usually a metal block on which the substrate, such as borosilicate glass, rests) and the relationship between the surface temperature of the glass while spraying and the block temperature has not been determined.[1] The heat transfer between two flat surfaces in contact is relatively poor, because contact actually exists only in a few isolated points on the two surfaces. The advantage of a liquid metal bath on which our substrate floats is that the molten metal is in intimate contact over all surfaces of the glass that it wets. We find that a bubble inadvertently trapped between the metal bath and the glass produces a significant difference in the deposit in the area where the bubble interfered with heat transfer. At high temperatures, deposition efficiency is lower, although other properties may be superior, and the deposit will be much thicker in the area where the heat transfer was poor.

Because different apparatus would have varying heat-transfer characteristics, it is important to know the effects of surface temperature as such, and we have calibrated our system accordingly. It is difficult to measure surface temperature with a thermocouple, because of the difference in cooling rates of the metal of the thermocouple and the surface of the glass. Therefore, we have chosen to measure the surface temperature radiometrically. The radiometric temperature measurement requires a knowledge of the surface emissivity. To have a surface of known emissivity, we have coated the glass with Grafilm, a graphite film manufactured by Asbury Graphite Films, Inc. The surface temperature was measured with a Raytek radiometer with nitrogen flowing onto the surface at the usual rates. To prevent overspray from coating the radiometer window, we did not have fluid flowing through the gun at the time; however, preliminary measurements show that cooling of the nitrogen flow

dominates the temperature and the effect of adding the liquid is insignificant in comparison with the much larger volume of gas. Figure 1 is the calibration curve for the radiometric surface temperature as a function of the solder bath temperature as determined by the controller setting.

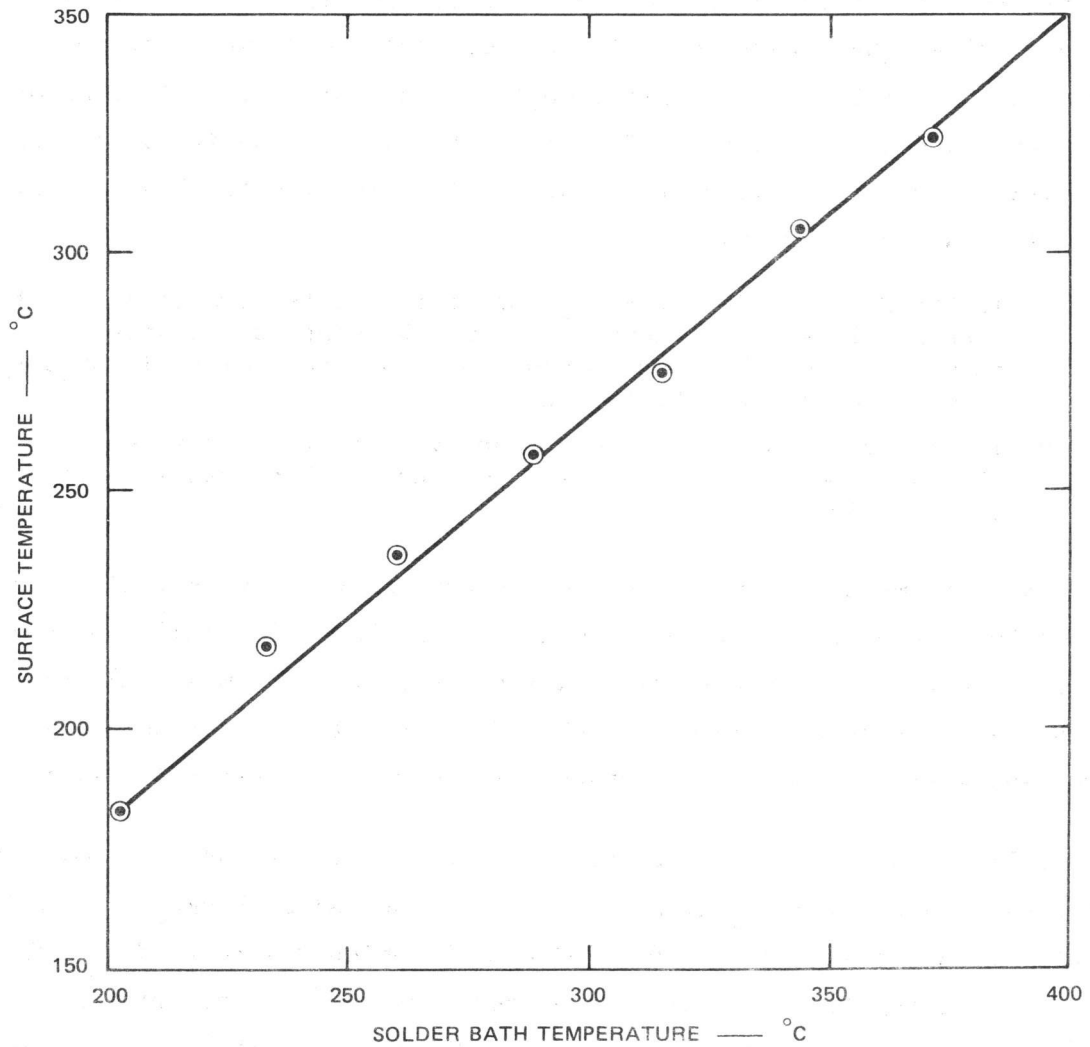

FIGURE 1 RADIOMETRIC SURFACE TEMPERATURE DURING SPRAYING AS A FUNCTION OF SOLDER BATH TEMPERATURE

B. Transparent Conductor

We have used three general types of transparent conductors: spray pyrolized tin oxide doped with antimony [SnO_2(Sb)], spray- pyrolized tin oxide doped with indium [SnO_2(In)], and sputtered indium tin oxide (ITO). Sprayed films were rapidly sprayed onto borosilicate glass substrates that had been heated to 600°C. Early attempts to deposit ITO by spray pyrolysis were unsuccessful. We were able to produce spray-pyrolized SnO_2 films with antimony doping with a minimum resistance of 200 ohms/□ and a transmission of 85 percent. We then modified the spray pyrolysis to produce a lower-resistance film. Two factors have contributed to lower resistance:

- If the HCl solution of $SnCl_4$ and additives is sprayed in short bursts, allowing the temperature of the glass substrates to return to 600°C between bursts, the resistance of antimony-doped films is as low as 100 ohms/□.
- If traces of indium are added, an even lower resistance is obtained, but at the expense of a considerable loss in optical transmission.

These films have a resistance of 20 ohms/□ and a transmission factor of 60 percent for unfiltered tungsten light at 100 mW/cm^2. With 1 percent antimony, the films are darker (40 percent transmission) and exhibit a sheet resistance of 200 ohms/□. These low-resistance films were used where the series resistance of the n-type contact is critical.

Films prepared by RF sputtering from a 94 percent indium/6 percent tin target in a 1:1/Ar:O_2 atmosphere at 4-μm Hg had a thickness of 650 angstroms, and resistance of 6 x 10^5 ohms/□ which was reduced to 100 ohms/□ by firing for 30 minutes in nitrogen at 450°C. The optical transmission of the conducting glass was 82 percent without and 78 percent with heat treatment.

C. Cadmium Sulfide (CdS)

1. Experimental Studies

Kazmerski et al.[2] have shown that the efficiency of CdS/$CuInSe_2$ cells is critically dependent on the resistivity of the CdS layer. We have resumed the examination of the deposition of CdS with the objective of lowering the resistivity. Thermodynamic studies show that a considerable excess of thiouruea is necessary for deposition of stoichiometric CdS. However, at least for undoped films, a deficiency of sulfur leads to a lower resistivity, as shown in Table 1.

Table 1

EFFECT OF Cd:S RATIO ON RESISTANCE
Substrate Temperature 225°C

Sample Number	Cd:S Ratio	Resistance (Ω/□)	Thickness (N)	Resistivity (Ω · cm)
5-34A	1:10	4×10^9	0.46	1.8×10^5
5-33A	1: 5	1×10^9	0.77	7.7×10^4
5-34B	1: 3	9×10^7	0.32 (.58)	2.8 (5.2) $\times 10^3$
5-33B	1:1.5	5×10^7	0.68	3.4×10^3
5-35A	1:1.1	1×10^7	0.56	5.6×10^2
5-35B	1:09	1.5×10^6	0.67	1.0×10^2

The heat treatment data of Marucchi et al.[3] show a drastic decrease in resistivity--and differing results--when nitrogen or hydrogen atmospheres are used. Our nitrogen treatment data (Table 2) are consistent with theirs (although we varied the time of heat-treating, rather than temperature) and show drastically decreased resistance (in the range of four orders of magnitude). Longer heat treatment restores these low values (Table 2).

Table 2

HEAT TREATMENT OF SPRAYED CdS FILMS IN N_2 AT 375°C

Sample Number	Cd:S Ratio	Temp. (°C)	Thick-ness (μm)	Resistance (Ω/□)						
				After Spray	Before Heat Treatment*	Heat Treatment				After Heat Treatment
						+5 min	+10 min	+15 min	+30 min	
5-40-C	1:0.9	325	0.3	6×10^7	6×10^7	3.7×10^3	–	–	–	3×10^3
5-40-B	1:0.9	305	0.6	4.7×10^7	7.5×10^9	–	–	4×10^8	–	2×10^9 †
5-40-B	1:0.9	305	0.6	4.7×10^8	1×10^8	7×10^5	1.5×10^5	6×10^4	1.5×10^5	1.5×10^5
5-30-C	1:1.5	230	–	$\sim 1 \times 10^8$	1.5×10^5	3×10^6	–	–	1.4×10^5	1.5×10^5
5-33-B	1:1.5	230	0.8	5×10^6	3.5×10^6	2×10^6	–	–	–	6.4×10^8
5-33-B	1:1.5	230	0.8	5×10^6	2.5×10^6	2.9×10^6	–	2.5×10^6	–	2.5×10^8
5-34-B	1:3	230	0.6	5×10^7	2×10^7	2×10^5	–	–	–	1.5×10^7
5-33-A	1:5	230	0.8	1×10^9	5×10^7	2×10^5	–	–	–	1.5×10^7

* The time in days between Cd:S deposition and heat tratment varied.

† Heat-treated at 400°C.

In the case of heat treatment in hydrogen, Marucchi et al.[3] show decreased resistivity as the temperature exceeds 400°C; our results, presented in Table 3, show that resistance increases(as in the case of nitrogen flow) after 30 minutes at 400°C or higher.

Table 4 clearly shows no significant difference in data from heat treatment in hydrogen and in nitrogen.

An aging effect on CdS films of sulfur-excess seems to be triggered by the annealing process. Although samples sprayed with a sulfur excess did show reduced resistivity immediately after heat treatment, the resistance returned in a few hours, in some cases even higher than the starting value (Tables 2 and 3). This result is similar to those of Ma[1].

The data in Table 5 show the reproducibility of the deposits at the various levels of cadmium excess and heat treatment in nitrogen at 375°C for five minutes. Some of the data are the same results reported in Table 3; in Table 6, these data are compared with identical firing conditions of a second piece of the sample for 10 minutes in nitrogen at 375°C. At Cd:S ratios less than 1:1, it appears that a 5-minute heat treatment results in lower resistivities.

Recent work has shown that sintering in cadmium vapor lowers the resistance of sintered CdS layers. Table 7 summarizes the heat treatment of spray-pyrolized CdS layers at 375°C and 400°C in nitrogen with a cadmium source in a boat just upstream from the sample. The drop in resistance did not occur at 375°C but at 400°C. [This could be a result of a different furnace geometry, since the sintering furnace is of two-inch diameter and the heat treatment furnace is less than one inch.] What is significant is that the resistance is a factor of five to ten lower than for nitrogen alone. More importantly, the resistance of one sample that had heretofore resisted heat treatment (Sample 7-5-A) was reduced more than five orders of magnitude in the presence of cadmium vapor. We do not know why Sample 7-5-A is different, unless it is

Table 3

HEAT TREATMENT OF SPRAYED CdS FILMS IN H_2 AT 375°C

Sample Number	Cd:S Ratio*	Resistivity (Ω•cm)						
		Before Heat Treatment	Heat Treatment					After Heat Treatment†
			+5 min	+10 min	+15 min	+30 min	+60 min	
7-5-E	1:0.7	2.7×10^{4}	9×10^{-1}	1.2×10^{0}	3.5×10^{0}	2.5×10^{1}	7×10^{1}	8.5×10^{1}
7-5-B	1:1	2.7×10^{5}	7×10^{1}	7×10^{1}	–	–	–	1.4×10^{5}
7-5-A	1:1	$> 5 \times 10^{5}$	2×10^{4}	–	1.3×10^{4}	–	–	1.3×10^{4}
7-5-D	1:0.9	2.5×10^{3}	3.1×10^{-1}	6.5×10^{0}	6.5×10^{0}	3.6×10^{0}	–	3.6×10^{0}
7-3-A	1:0.9	1.7×10^{4}	5.5×10^{-1}	3.2×10^{-1}	1.2×10^{0}	–	–	9×10^{-1}
7-6-B	1:0.75	6×10^{5}	6×10^{1}	–	–	–	–	6×10^{1}

*All samples sprayed at a Sn-Pb bath temperature of 370°C.

†Measured 10 days later.

Table 4

COMPARISON OF THE FIVE-MINUTE HEAT TREATMENTS IN N_2 AND H_2 AT 375°C*

Sample Number	Cd:S Ratio	Resistance (Ω/□)			
		Nitrogen Treatment		Hydrogen Treatment	
		Before	+5 min	Before	+5 min
7-5-B	1:1	3×10^9	6.5×10^5	5.9×10^9	1.4×10^6
7-5-A	1:1	3×10^{10}	3×10^9	10^{10}	4×10^8
7-3-A	1:0.9	5×10^8	6×10^4	3.4×10^8	1.1×10^4
7-5-D	1:0.8	2.3×10^7	8.3×10^3	5×10^7	6.3×10^3
7-5-E	1:07	5.1×10^8	1×10^5	5.4×10^8	1.8×10^4

* The starting value differ slightly, because the samples for heat-treatment are cut from different areas, but from the same film.

Table 5

FIVE-MINUTE HEAT TREATMENTS AT 375°C OF CdS FILMS OF DIFFERENT Cd:S RATIOS UNDER N_2 FLOW

Sample Number	Ratio (Cd:S)	Resistance (Ω/□)	
		Before	+5 min
7-5-E	1:0.7	5.1×10^8	1.0×10^5
7-6-C	1:0.7	5.0×10^8	5.0×10^5
7-6-A	1:0.75	1.0×10^{10}	3.0×10^7
7-6-B	1:0.75	1.3×10^8	1.1×10^8
7-5-C	1:0.8	1.0×10^9	2.0×10^6
7-5-D	1:0.8	2.3×10^7	8.3×10^3
7-6-D	1:0.85	2.0×10^9	3.0×10^6
7-6-E	1:0.85	8.0×10^8	5.0×10^6
7-3-A	1:0.9	5.0×10^8	6.0×10^4
7-3-B	1:0.9	1.5×10^8	4.0×10^4
7-10-A	1:0.95	1×10^8 - 1×10^9	5.0×10^5
7-10-B	1:0.95	6.0×10^8	2.0×10^5
7-5-A	1:1	3.0×10^{10}	3.0×10^9
7-5-B	1:1	3.0×10^9	6.5×10^5

Table 6

RESISTANCE OF CdS FILM AFTER FIVE- AND TEN-MINUTE HEAT TREATMENTS IN N_2 AT 375°C

Sample Number	Cd:S Ratio	Resistance (Ω/□)			
		Before	+5 min	Before	+10 min
7-5-B	1:1	3×10^9	6.5×10^5	7×10^8	2×10^5
7-5-A	1:1	3×10^{10}	3.0×10^9	2×10^{10}	4×10^8
7-3-A	1:0.9	5×10^8	6.0×10^4	3×10^8	1×10^5
7-5-D	1:0.8	2.3×10^7	8.3×10^3	2×10^7	1×10^4
7-5-E	1:0.7	5.1×10^8	1.0×10^5	4×10^8	2×10^5

Table 7

HEAT TREATMENT OF SPRAYED CdS FILMS IN CADMIUM VAPOR

Sample Number	Cd:S Ratio	Resistance (Ω/□)			
		Before	+5 min (375 °C)	+10 Min (375 °C)	+10 Min (400 °C)
7-3-A	1:0.9	3×10^8	3×10^8	6.4×10^7	1.7×10^3
7-5-A	1:1	1.5×10^{10}	9×10^9	1.3×10^{10}	2.5×10^4
7-5-B	1:1	2×10^8	3×10^7	2.1×10^8	1.2×10^3
7-5-D	1:08	8×10^6	1.5×10^7	1.4×10^6	5.1×10^2
7-5-E	1:07	2×10^8	2×10^7	2.8×10^7	3.0×10^3

significant that it was left in the deposition chamber for as much as 30 minutes after the spray solution was exhausted.

The electrical measurements are made very simply through a pair of 1 x 0.5 cm^2 aluminum contacts on a resilient pad, and thicknesses were measured with the SEM. Data with the same sample number in the "Before" columns in Table 4 are from two portions cut from a single, sprayed-glass plate, and include the real difference in resistance, along with the precision of the measurement itself.

The studies summarized in Tables 1 through 6 lead to the following general conclusions:

- Nitrogen is at least as effective as hydrogen for heat treatment.
- The $CdCl_2$:thiouruea ratio (Cd:S) in the spray solution is critical, in that samples prepared from solutions with an excess of thiouruea have not been converted to a stable low resistance by heat treatment, while stable heat-treated resistances have resulted for Cd:S greater than 1:1.
- Heat treatment in nitrogen at 375°C for 5 minutes is sufficient, while periods of more than 10 minutes result in higher resistances.
- Heat treatment in a nitrogen atmosphere containing cadmium vapor is superior to nitrogen alone.

2. Physical Properties

We have studied the physical properties of spray-pyrolized CdS films. A number of studies have been reported in the literature, but none have related heat treatment and spray solution composition to film resistivity. We have studied some of the films that were described in the preceding pages using XRD, TEM, and the Read camera (a modified Debye-Scherer with the linear dimension of the cylinder increased to intersect a larger cross section of the diffraction cones).

Table 8 summarizes the results of the XRD study of a series of films sprayed from solutions of varying Cd:S concentration ratios. The crystallinity is expressed in terms of hexagonality or the ratio of the

Table 8

DARK RESISTIVITY AND HEXAGONALITY
OF FILMS WITH VARIOUS Cd:S RATIOS
Substrate temperature 225°C; spray rate 0.05 cm^3/s

Sample	Cd:S Ratio	Dark Resistivity (Before Heat Treat) ($\Omega \cdot cm$)	Hexagonality
5-34A	1:10	2×10^5	0.77
5-33A	1:5	7.8×10^4	0.52
5-34B	1:3	2.8×10^3	0.56
5-33B	1:1.5	3.3×10^3	0.46
5-35A	1:1.1	5.5×10^2	0.46
5-35B	1:0.9	9.1×10	0.47

hexagonal to cubic CdS phases present in the as-deposited films. Because the XRD patterns differ only slightly for hexagonal and cubic CdS, it is necessary to use the Smith-Short equation[4,5] as developed by Ma[1] to estimate the ratio. We have also examined the films with the TEM. At high magnification (220,000X), we estimated the crystallite size of the heat-treated film Sample 5-40-CHT (Table 2) to be 300 angstroms. Microdiffraction patterns from a number of crystallites showed the hexagonal structure; the hexagonality from XRD was greater than 0.7. Read camera studies showed that this sample was highly oriented. A second portion of Sample 5-40-C that was not heat treated also is oriented.

Another film (Sample 5-35-B in Table 1) that was also sprayed from a 1:09 Cd:S ratio solution showed an XRD hexagonality of 0.47. It was sprayed at a substrate temperature of 225°C (compared to 325°C).[1] The TEM showed 500 angstroms to 1 μm grain size for Sample 5-35-B. The Read camera showed no preferred orientation, as expected from the cubic phase. Microdiffraction also showed the presence of cubic phase.

These results show that the crystal structure of spray-pyrolized CdS is influenced by both the solution composition and the substrate temperature.

D. Copper Indium Sulfide ($CuInS_2$)

The objective of the spray pyrolysis program is a $CdS/CuInSe_2$ cell. However, because the starting sulfur compound, N,N'-dimethylthiouruea, is chemically stable relative to the corresponding selenium compound, the preliminary studies were with the $CuInS_2$.

$CuInS_2$ films were sprayed from aqueous solution starting with a solution of CuCl dissolved in HCl and diluted with water to a concentration of 0.005 molar. A molar equivalent of $InCl_3$ was added, together with the desired quantity of N,N'-dimethylthiouruea. For the first series of films, the In:Cu ratio was 1:1. The In:S ratio was varied from 0.5 to 1.6. Table 9 summarizes the conditions for preparation of six films. Sample 2-13-A was prepared at a surface temperature of 230°C. The third column of the table shows the In:S ratios for the various films and the fourth column the quantity of indium and copper deposited on each substrate.

1. X-Ray Fluorescence Measurements

All of the films were analyzed by X-ray fluorescence techniques using the energy dispersive X-ray fluorescence analyzer (EDAX) in the scanning electron microscope. Because quantitative standards of $CuInS_2$ were not available, the data in Table 10 are presented as ratios to the indium intensity. The S:In ratio is relatively constant when sulfur content exceeds 0.5. Copper:indium intensity ratios are very near 0.5, except that copper is low when In:S ratio is 1:2. The chlorine content of the first four films was rather constant (ranging from 0.1 to 0.3);

Table 9

SUMMARY OF $CuInS_2$ SPRAY-PYROLIZED FILMS

Layer	Temperature (^oC)	In:S	Moles Sprayed	X-Ray Intensity Ratios		
				S:In	Cu:In	Cl:In
2-13	230	1/2	1×10^{-4}	0.76	0.34	0.24
2-14A	220	1/2	2.5×10^{-4}	1.19	0.46	0.12
2-18C	220	1/3	6.2×10^{-4}	1.94	0.5	0.30
2-18D	220	1/6	6.2×10^{-4}	1.45	0.48	0.23
2-21A*	220	1/2	6.2×10^{-4}	0.91	0.34	0.94
2-31*	220	1/4	6.2×10^{-4}	1.89	0.49	0.00

* Spray solution contained $NH_2OH.HCl$.

Table 10

OXYGEN CONTENT IN $CuInS_2$ DETERMINED BY WAVELENGTH DISPERSIVE X-RAY (SEM)

SiO_2 Standard		Layer 2-31		Layer 2-18D	
Counts*	Percent Oxygen†	Counts*	Percent Oxygen†	Counts*	Percent Oxygen†
27059	66.7	347	0.86	2363	5.82
27292	66.7	393	0.96	2487	6.08
28136	66.7	368	0.87	2417	5.73

* Counts are corrected for background.

† Oxygen content expressed in atomic percent.

however, Sample 2-21-A [which was sprayed with a solution containing hydroxylamine hydrochloride ($NH_2OH \cdot HCl$) in air] contained an excess of chlorine, verified by the Auger analysis (discussed later). Sample No. 2-2 was prepared in the spray chamber designed for nitrogen spraying, excluding most of the air and lowering the oxygen content of the film. An unexpected result of this experiment was the absence of detectable chlorine in the film, although the S:In and Cu:In ratios were similar to the other films.

The efficiency of the nitrogen spray apparatus in lowering the oxygen content of the films is shown in Table 10, which lists the oxygen content, as determined by X-ray fluorescence using the wavelength-dispersing attachments in the SEM. Because there are no adequate direct standards, a sample of fused quartz was used as a standard in the first column, which shows the number of counts for the SiO_2 standard, which has an oxygen content of 66.7 atomic percent. For Sample 2-31 ratioed to the number of counts for the silicon standard, we calculate an oxygen content of approximately 0.9 atomic percent. for a layer sprayed in air (Sample 2-18-D), the oxygen content is approximately 6 atomic percent. These oxygen contents are not accurate, but they are a clear measure of the effects of nitrogen in excluding oxygen from the growing films. The structure of the spray apparatus is such that in the fume hood where it is located there is a sufficient draft for some air to be moved under the spray chamber and consequently the deposit 2-31 was not of uniform thickness from the front to the back of the chamber. A secondary outer enclosure was constructed to prevent a draft from affecting this deposition and to aid in preventing back diffusion of oxygen into the chamber; thus, it is hoped that the oxygen content of future films will even be lower than that of Sample 2-31.

2. Auger Analysis

Table 11 presents the analysis by Auger spectrometry of the surface and after-argon sputtering to a depth of 1000 angstroms for four samples. Figure 2 is an Auger depth profile of Samples 2-21-A. These

Table 11

AUGER ANALYSIS AT SURFACE(S) AND 1000 Å(B)

Sample Number	Sulfur		Carbon		Indium		Oxygen		Copper		Chlorine	
	S	B	S	B	S	B	S	B	S	B	S	B
2-14A	46	203	152	0	138	171	107	109	78	57	12	24
2-18C	81	213	158	0	60	93	42	16	41	66	78	84
2-18D	19	165	185	0	59	92	52	26	29	25	178	50
2-21A	15	47	114	18	80	125	53	49	29	16	246	463

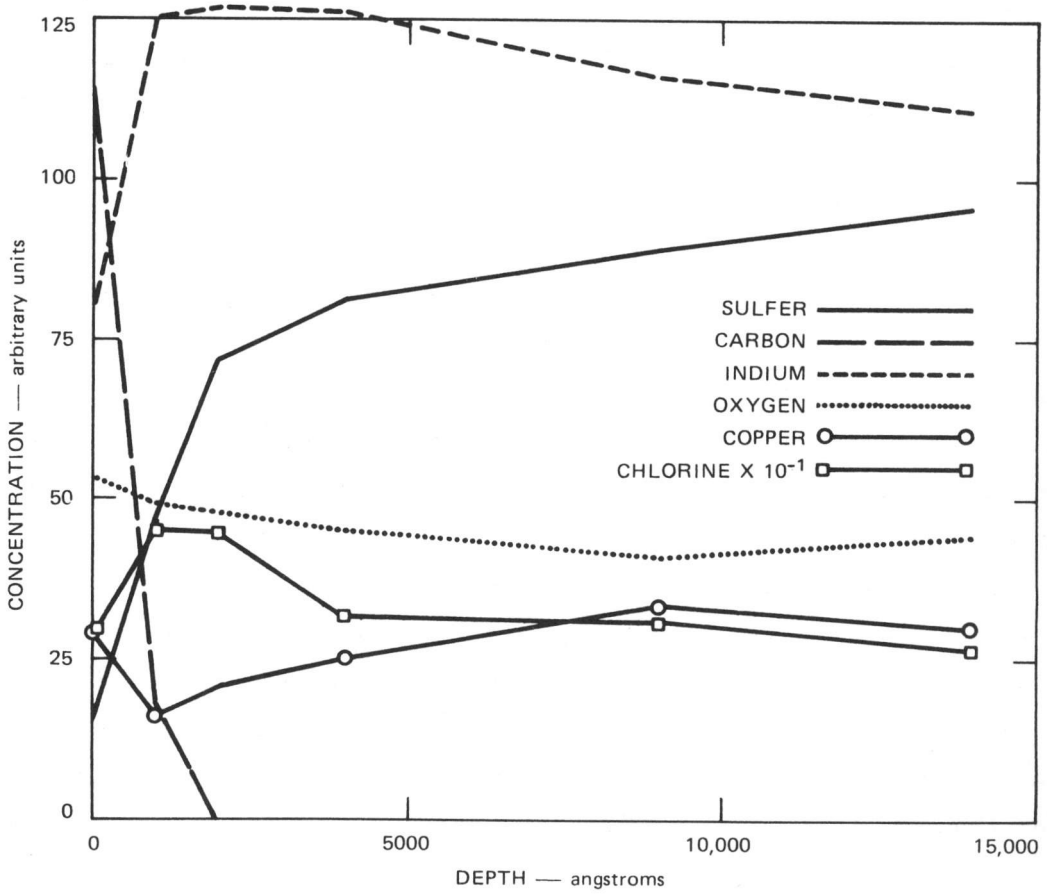

FIGURE 2 AUGER DEPTH PROFILE OF SAMPLE 2-21A

results show surface contamination with carbon, a generally low value for indium on the surface, and the high chlorine content of Sample 2-21-A in agreement with the X-ray fluorescence results in Table 10.

Figure 2 shows the depth profile of Sample 2-14-A to about 4 μm, which is the interface, although this was not sharply delineated by further sputtering. This shows the carbon and low sulfur on the surface, and an irregularity of indium and copper near the surface. These results agree with the XPS data, which indicate a high In:Cu ratio. Figure 2 shows the very high chlorine content of Sample 2-21-A, a much higher Cu:In ratio throughout the film than found in Sample 2-14-A. All samples indicate that the In:Cu ratio is high. All but Sample 2-18-C show copper drops and indium rises in the first 1000 angstroms.

Other major variables studied were

- Spray rate
- Total volume of solution sprayed
- Ratios of copper to indium and sulfur to indium in the spray solution.

Based on the Auger spectroscopy studies and XPS studies, it was determined that an excess of copper in the spray solution improves the stoichiometry of layers; the effects of an excess of sulfur were also studied. Table 12 summarizes the conditions of preparation and some results for the thin films.

The Kevex X-ray fluorescent system on our scanning electron microscope has a computer and disc storage facility; using this arrangement, the computer can determine (with an accuracy much greater than that obtained by measuring peaks on a CRT display) the total number of counts attributable to a given element. Because standard samples were not available to calibrate the X-ray unit, the values in Table 12 are not concentrations in weight or atomic percent.

Figure 3 shows a scanning electron micrograph of the surface of Sample 2-65, together with a CRT display of the X-ray fluorescence.

Table 12

SUMMARY OF THE EFFECT OF CONCENTRATION RATIOS ON $CuInS_2$ DEPOSITS

Layer	Moles x 10^{-4}	Spray Conditions		Tin-Bath (°C)	Concentration Ratios		X-ray-Derived Intensity Ratios			Oxygen Content (percent)	Comment
		Rate (ml/h)	Total (ml)		Cu:In	S:In	Cu:In	S:In	Cl:In		
2-43	3.1	120	50	300	1:1	4:1	0.47	1.38	0.29	9.4	$NH_2OH \cdot HCL$
2-44	3.1	85	50	280	1:1	4:1	0.50	1.50	0.37	10	$NH_2OH \cdot HCL$
2-45	6.2	300	100	250	1:1	4:1	--	--	--	-	$NH_2OH \cdot HCL$
2-46	12.4	300	200	280	1:1	4:1	0.79	2.24	0.18	1.4	$NH_2OH \cdot HCL$ (last time)
2-47	12.4	110	200	280	1:1	4:1	0.63	2.35	0.07	1.3	Metering pump introduced
2-48	12.4	130	200	280	1:1	4:1	--	--	--	-	Film flaked
2-49	12.4	40	200	280	1:1	4:1	0.70	2.53	0.07	4.7	Slow metering
2-50	12.4	40	200	280	1.5:1	10:1	0.83	2.30	0.03	6.1	
2-62	12.5	47	200	265	1.5:1	10:1	2.11	3.60	0.00	-	Crystals
							0.74	2.52	0.09	-	Matrix
2-63	12.5	50	200	270	1.5:1	10:1	1.67	3.34	0.00	-	Crystals
							0.75	2.69	0.08	-	Matrix
2.65	27	115	350	285	1.5:1	10:1	0.78	2.37	0.00	-	Average
							4.57	4.05	0.00	-	Crystals
							0.68	2.27	0.00	-	Matrix
2-71	32	135	400	270	1.5:1	8:1	0.91	2.67	0.03	-	Average

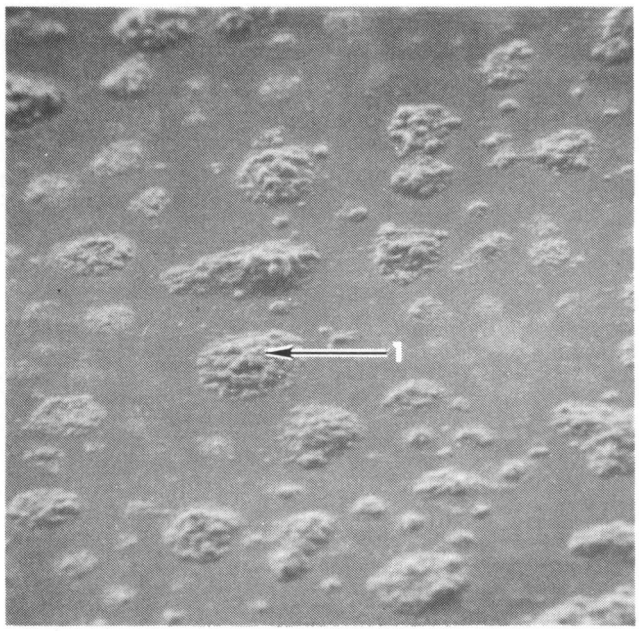

(a) 500× VIEW OF SURFACE

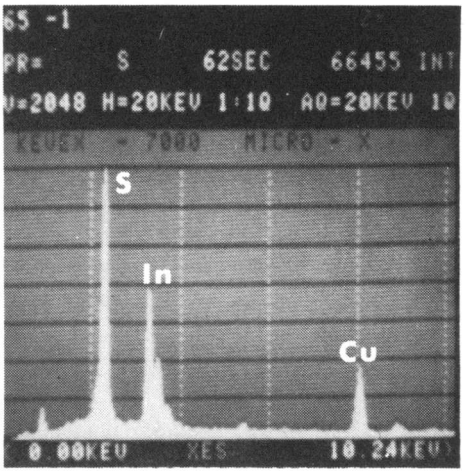

(b) X-RAY FLUORESCENCE READOUT FROM (a)

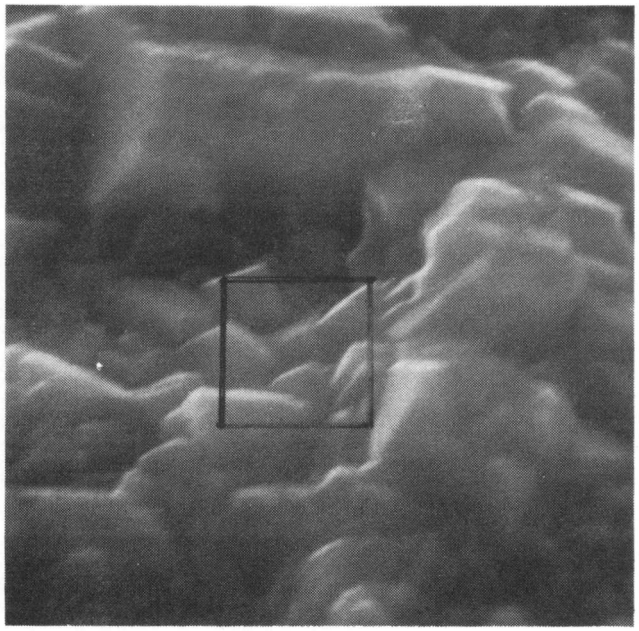

(c) 10,000× VIEW OF AREA 1 IN (a)

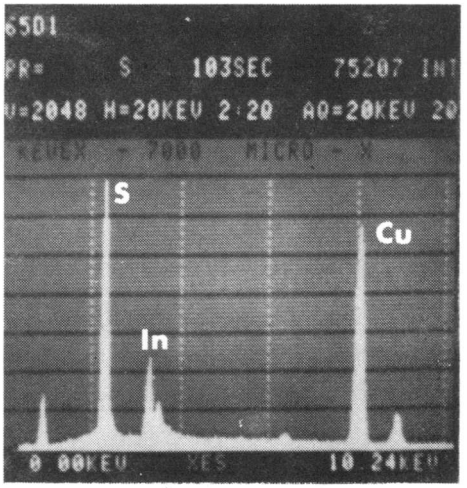

(d) X-RAY FLUORESCENCE READOUT FROM (c)

FIGURE 3 SCANNING ELECTRON MICROGRAPH AND X-RAY FLUORESCENCE DATA FOR SAMPLE 2-65

Figure 3(a) is a SEM photograph at 500X showing clusters of crystallites on a relatively smooth surface. (In the discussion that follows, we refer to these clusters as "crystals" and to the smooth surface as the "matrix".) The CRT display in Figure 3(b) shows the entire area that has been sampled with X-ray fluorescence to produce an "average" analysis for both the crystal and the matrix. Figure 3(c) is a 10,000X magnification of the area indicated in Figure 3(a) by the numeral 1; the square scribed on Figure 2(c) is an area subsequently investigated at 50,000X, reported later in this discussion. Figure 3(d) is the CRT display corresponding to the area in Figure 3(c). In these panels, comparison of the relative heights of the peaks for copper and indium shows that the crystals are relatively rich in copper and deficient in indium.

Table 13 summarizes a similar analysis of spray-pyrolized $CuInS_2$, including samples that were heat-treated in H_2S. The data in Table 13 are ratios of the X-ray-derived counts for copper:indium, sulfur:indium, and copper:sulfur. Again, these data do not represent concentrations in terms of weight percent, or atomic percent, but rather the number of counts for copper kα and indium Lα. Because standard samples of $CuIns_2$ are not available with which to calibrate the apparatus, these data cannot be presented in terms of absolute concentrations. Despite this limitation, it is clear that the matrix has a different composition than the crystals, and that the matrix is similar from sample to sample: The crystals are rich in copper and sulfur and deficient in indium. The matrix was analyzed at 2,000X magnification; the crystals were analyzed at 10,000X, and individual crystals at 50,000X. Treating the samples in 20 percent H_2S in nitrogen at 300°C for one hour increased the copper and sulfur content of the crystals, and decreased the indium.

Figure 4 shows some of the results of a SEM X-ray fluorescence investigation of Sample 2-65, which had been etched for 75 seconds in concentrated nitric acid. This etching was undertaken to study the bulk of the chemically sprayed layer by XPS. Examination with the SEM revealed that the matrix areas were etched, but that the crystal areas had been attacked selectively, thereby producing what we refer to as a

Table 13

X-RAY MICROANALYSIS OF $CuInS_2$, INCLUDING HEAT TREATMENT

Sample Number* and Area	X-ray-Derived Intensity Ratio		
	Cu/In	S/In	Cu/S
49			
Matrix	0.70	2.53	0.28
Matrix	0.63	1.97	0.32
Matrix	0.87	1.32	0.50
Crystals	1.32	3.18	0.42
Crystals	1.10	2.90	0.38
49HT			
Matrix	0.59	1.19	0.49
Crystals/	3.72	6.96	0.53
50			
Average	0.83	2.30	0.36
50HT			
Average	0.92	2.77	0.33
62			
Matrix	0.74	2.52	0.29
Crystals	2.11	3.60	0.59
62HT			
Matrix	0.81	2.71	0.30
Matrix	0.83	2.70	0.31
Crystals	1.54	3.21	0.48

Sample Number* and Area	X-ray-Derived Intensity Ratio		
	Cu/In	S/In	Cu/S
63			
Matrix	0.75	2.69	0.28
Crystal	1.67	3.34	0.45
63HT			
Matrix	0.69	2.32	0.30
Matrix	0.72	2.57	0.28
Crystal	2.55	4.10	0.62
65			
Average	0.78	2.37	0.33
Matrix	0.68	2.27	0.30
Matrix	0.65	2.17	0.30
Crystals	4.57	4.05	1.13
Crystals	2.00	3.61	0.55
Crystals	2.59	3.73	0.69
Crystals	5.89	5.23	1.13
Crystals	5.82	7.09	0.82
71			
Average	0.91	2.67	0.34
71HT			
Average	0.86	2.50	0.35

*HT suffix indicates heat treatment of one hour at 300°C in 20 percent H_2S in N_2.

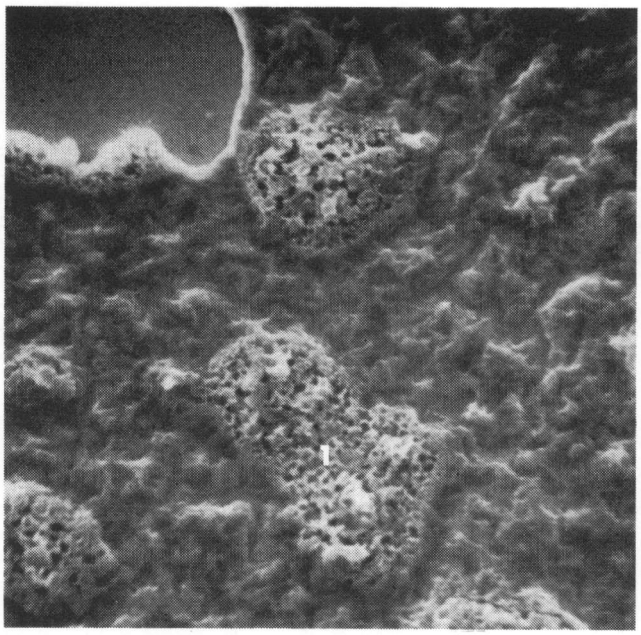

(a) 2000× VIEW OF SURFACE

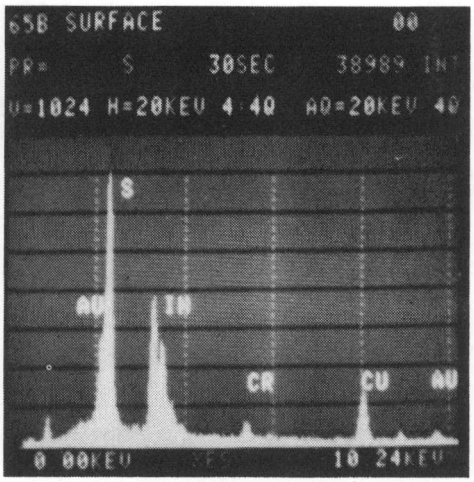

(b) X-RAY FLUORESCENCE READOUT FROM (a)

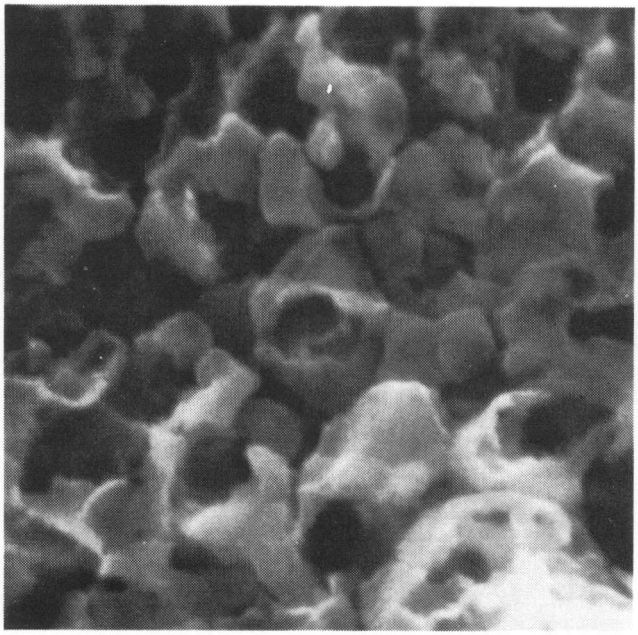

(c) 10,000× VIEW OF AREA 1 IN (a)

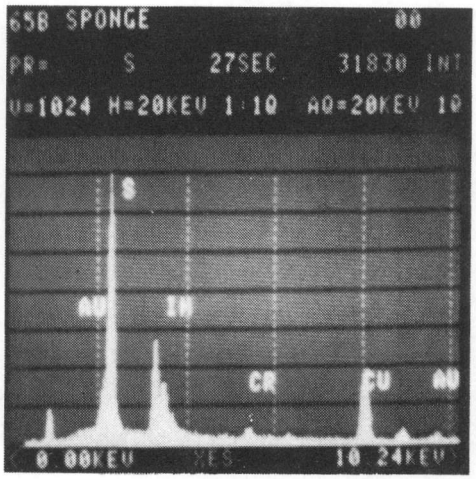

(d) X-RAY FLUORESCENCE READOUT FROM (c)

FIGURE 4 SCANNING ELECTRON MICROGRAPH AND X-RAY FLUORESCENCE DATA FOR SAMPLE 2-65 FOLLOWING 75 SECONDS OF ETCHING IN HNO_3

"sponge" material. Figure 4(a) is a 2,000X view of the surface, showing the spongy areas as well as the degree of attack on the matrix. Figure 3(b) is a CRT display of X-ray fluorescence for an area of the matrix; the distribution of copper, indium, and sulfur is similar to what was seen in figure 3(b) for Sample 2-65. Figure 4(c) is a 10,000X view of one of the sponge areas; the selective attack on the crystals is clearly visible. Figure 4(d), the CRT display corresponding to Figure 4(c), is remarkably similar to Figure 4(b) and demonstrates that the remaining material is of the same composition as the matrix.

In summary, the data in Table 13 and Figures 3 and 4 indiate that, under the conditions of spray in which the copper:indium ratio is 1.5:1 and the sulfur:indium ratio is of the order of 10:1, there is a tendency for the growth of isolated crystals of Cu_xS (possibly alloyed with an indium compound); however, the data for Sample 2-49 also indicate that the crystals are copper-rich, even when the copper:indium ratio in the spray solution is 1:1. The fact that the heat treatment sometimes increases the copper content of the crystals (or decreases the indium) is in agreement with the results of thermodynamic studies that indicate that the sulfur pressure for In_2S_3 is greater than that for Cu_2S.

Thermodynamic studies (see Section VI) showed that an H_2S atmosphere would be more effective in converting the indium oxide to indium sulfide, but that the vapor pressure considerations also suggested that 300°C was probably the ideal temperature for this kind of heat treatment. Table 14 summarizes the heat treatment for five samples, listing the heat treatment conditions and the measured conductivity for the samples before and after treatment. The heat treatment did not affect the crystallinity of the films; X-ray diffraction patterns taken on one sample after treatment were not different from those taken before.

Figure 5 is the Auger profile for Sample 2-50, showing the intensities of the various elements normalized to indium and corrected for Auger yield on the basis of spectra in the PEI Handbook.[6] Because of the number of elements included in this chart, these distributions are somewhat difficult to follow. Accordingly, we have replotted the important

Table 14

EFFECT OF HEAT TREATMENT ON THE RESISTANCE OF $CuInS_2$ FILMS

Sample Number	Heat Treatment Conditions			Sheet Resistance (Ω /□)	
	Temperature (°C)	Time (min)	H_2S Concentration (percent)	Before Heat Treatment	After Heat Treatment
2-50	300	60	10	4,000	2,000
2-62	300	60	10	60	50
2-63	300	60	20	150	60
2-65	400	30	20	60	250
2-71	300	60	25	5	15

elements of copper, sulfur, and indium in Figure 6. Even from Figure 5 it is obvious that the oxygen content on the surface is very high and the sulfur content very low. The substrate/glass interface to the $CuInS_2$ is not well defined. From the preceding discussion, it is clear that these layers are not entirely uniform and that some components of the crystalline mixture must be sputtered more rapidly than others such that "holes" appear in the deposit near the interface. Consequently, the signals for the barium and oxygen of the substrate glass appear to rise over a fairly great depth as the holes open, while the copper, indium, and sulfur intensities drop off relatively slowly as the remaining deposit is removed.

Figure 6 presents the Auger peak ratios for the same sample (2-50) in the form of copper:indium and sulfur:indium ratios. From these plots it is apparent that, although the surface is low in sulfur, most of the bulk is higher than the theoretical level for $CuInS_2$ of 2.0. Although the surface is somewhat deficient in copper, after the first 1000 angstroms, the copper concentration exceeds the indium. From this it is clear that the solution's copper:indium ratio of 1.5:1 is excessive, as is the sulfur:indium ratio of 10:1.

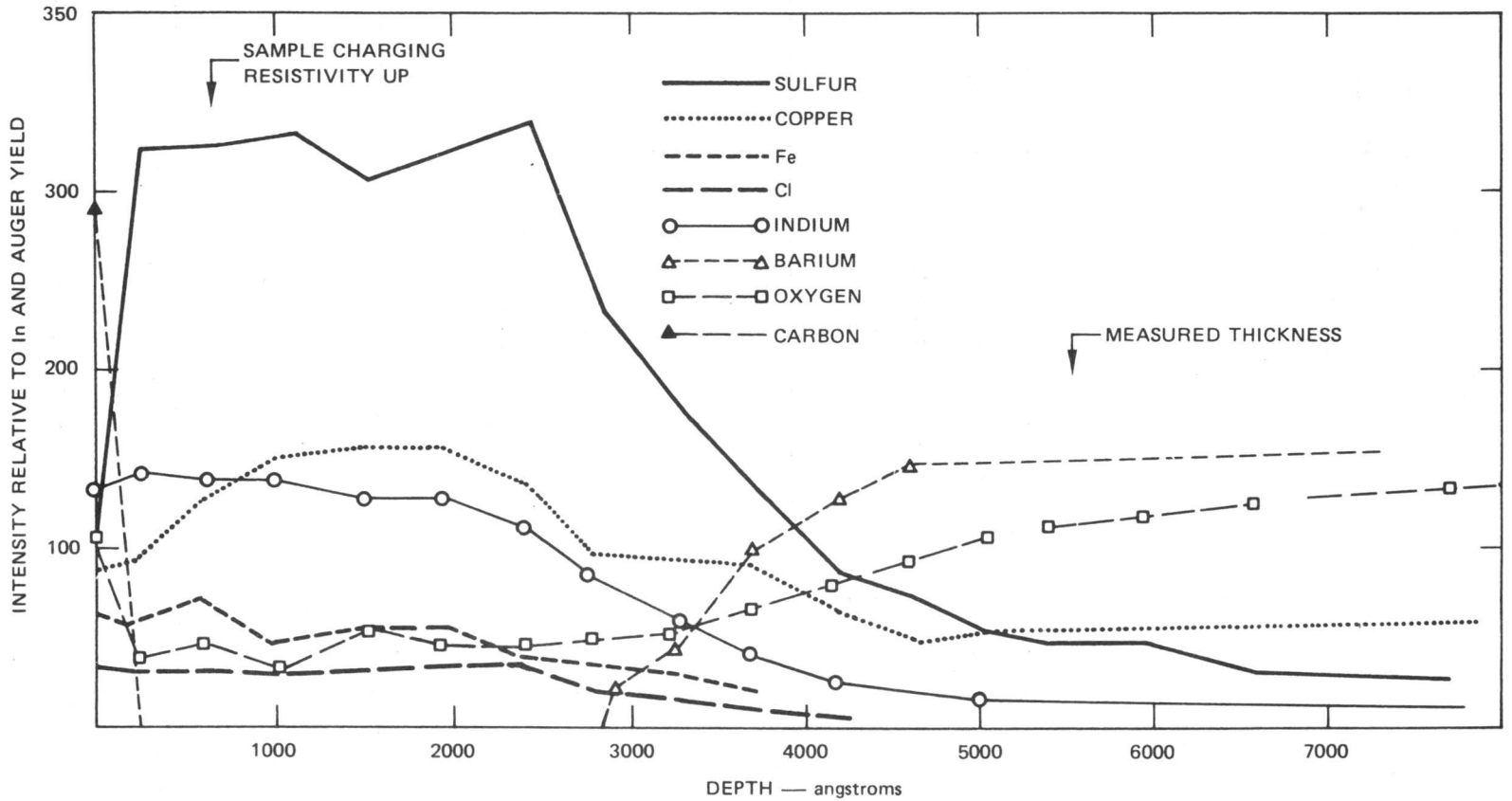

FIGURE 5 AUGER PROFILE FOR SAMPLE 2-50

Cu/In = 1.5/1; S/In = 10/1.

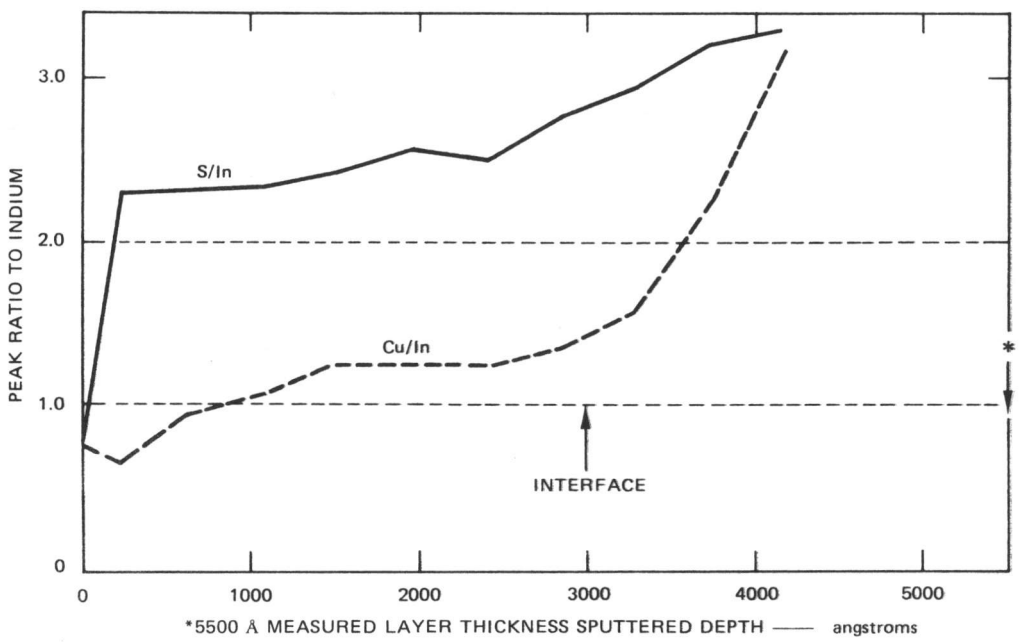

FIGURE 6 AUGER PEAK RATIOS FOR SAMPLE 2-50

Solution concentrations: Copper to Indium 1.0:1;
Sulfur to Indium 2.0:1

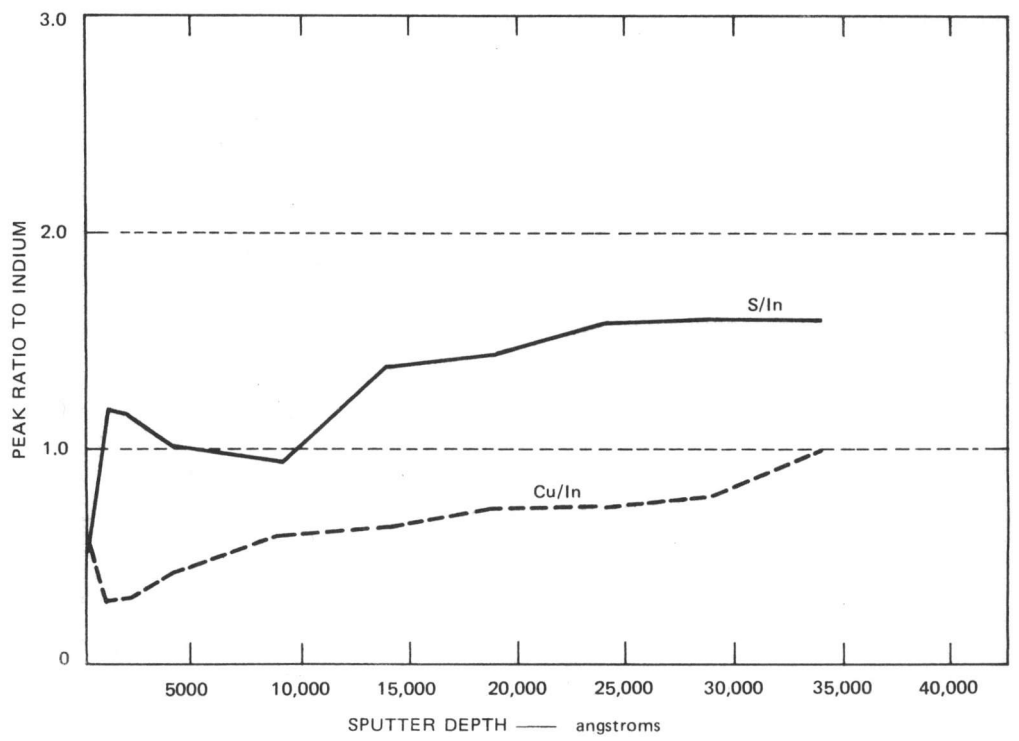

FIGURE 7 AUGER PEAK RATIOS FOR SAMPLE 2-14A

Solution concentrations: Sulfur to Indium 2.0:1;
Copper to Indium 1.0:1

Figure 7 is a similar reduction of data for Sample 14-A. The solution concentrations for Sample 2-14-A were the theoretical values of a 1.0:1 copper:indium ratio and a 2.0:1 sulfur:indium ratio. Figure 7 shows that under those circumstances, sulfur and copper concentrations are both low in the bulk and that the sulfur ratio is still very low on the surface. However, upon sputtering well into the layer near the interface, the copper rises to near the theoretical value of 1.0:1 and the sulfur reaches 1.6:1, which is closer to the theoretical value of 2.0:1.

These average values do not represent a uniform homogeneous film, since the SEM analyses show a segregation of the copper and sulfur in surface crystals. However, it remains clear that the composition near the glass interface is closer to theoretical than it is on the surface and that, as the layer grows, the ratios drift off the stoichiometric value. The low sulfur content of almost all surfaces studied to date using both Auger analysis and XPS shows a tendency for the surface to oxidize after it is removed from the nitrogen atmosphere in which it was prepared.

E. Copper Indium Selenide ($CuInSe_2$)

Copper forms an insoluble complex with N,N′-dimethylselenourea (DMSeU), and a precipitate forms in solutions of CuCl, $InCl_3$, and DMSeU in 10 to 15 minutes after preparation. It is possible to spray films using small increments of these chemicals mixed immediately prior to spraying. We have found that the copper-DMSeU precipitate will dissolve in an alcoholic solution; the minimum effective concentration is 30 percent ethanol. Acetone and isopropanol are not as effective as ethanol. The solution of 30 percent ethanol is not flammable. X-ray fluorescence analysis of a precipitate from a CuCl, $InCl_3$, and DMSeU solution showed that the precipitate was the copper-DMSeU complex, and did not contain a significant amount of indium.

Aqueous DMSeU solutions are photosensitive and decompose to precipitate selenium in room light. The reaction is inhibited in the $CuCl/InCl_3$ solutions, and it appears that the HCl incorporated into the solution to increase the solubility of these salts forms a hydrochloride with the amine groups of the DMSeU stabilizing of the C=Se bond.

A number of films have been sprayed using the alcoholic solution. The preparation conditions and the X-ray fluorescence analysis of four of these films and two sprayed from the instable aqueous solutions are summarized in Table 15. The X-ray fluorescence analysis was calibrated with a sample of $CuInSe_2$ generously supplied by Prof. J.J. Loferski and R. Beaulieu of Brown University. The analysis is expressed in terms of stoichiometry, with indium arbitrarily assigned a subscript of unity. The extent to which the copper and selnium subscripts deviate from the stoichiometric values of one and two respectively, is a measure of the nonstoichiometry. If both are significantly above stoichiometry, the sample is indium-deficient.

The analytical results in Table 15 include a result for one of the crystalline growths on Sample 4-19 similar to those observed for $CuInS_2$ (see Figure 3). In this case, the crystallite is rich in copper, but not in selenium (as would be expected from the results with the sulfur compound). The explanation for this may be found in the thermodynamics (Section VI). The presence of excess H_2Se (from DMSeU) will lead to free selenium in the film, and CuSe is thermodynamically preferred over Cu_2Se. The data in Table 15 and the thermodynamic studies show clearly that the excess of the chalconide that favored stoichiometry for $CuInS_2$ should be avoided in the case of the selenide. Yet, the thermodynamics indicate that there is a tendency toward residual chlorides as the excess of the DMSeU is decreased toward the stoichiometric value. However, Cu_2Se is also favored. Obviously, there are competing reactions and the ideal situation will have to be determined experimentally. the excess selenium will certainly be less than the factor of five that was used for sulfur. These conclusions are supported by the optical absorption studies (see Section VI).

Table 15

SUMMARY OF $CuInSe_2$ FILMS

Sample Number	Spray Conditions		Tin-Bath Temperature (^oC)	Concentration Ratio (Cu:In:Se)	X-Ray Analysis (Relative to In)	Comments
	Rate (ml/h)	Total (ml)				
4-5B	60	100	230	1:1:2	$Cu_{0.65}InSe_{1.9}$	No alcohol
4-6	60	100	230	1:1:2	$Cu_{0.68}InSe_{1.82}$	No alcohol
4-6B	60	30	230	1:1:4	$Cu_{1.2}InSe_{2.7}$	Alcohol
4-19M	100	106	230	1:1:6	$Cu_{1.7}InSe_6$	Alcohol
4-19X	--	--	--	--	$Cu_{3.6}InSe_4$	Alcohol
4-26	60	375	260	1:1:6	$Cu_{0.93}InSe_{3.7}$	Alcohol
4-28	60	375	266	1:1:6		Alcohol
4-28HT	--	--	--	--	$Cu_{1.2}InSe_{3.0}$	

Table 15 also shows the effect of heat treatment of a sprayed film. A portion of film Sample 4-28 was sealed in an evacuated quartz ampule with a slight excess of selenium and heat treated at 600°C for 16 hours. Although the X-ray fluorescence results indicate no significant change in the elemental composition upon heat treatment, X-ray diffraction (Figure 8) shows that the crystal size was increased.

Figure 8 includes diffraction patterns for some of the other samples listed in Table 15 and a pattern for the standard sample from Brown University. The poor crystallinity of Sample 4-6-B is related to the rapid spraying that was required by the instable aqueous solution. The lines for sphalerite $CuInSe_2$ are present, but other lines are attributed to $CuSe_2$. The fact that Sample 4-28 exhibits a better X-ray diffraction pattern than does Sample 4-26 can not be explained by any difference in their preparation. The deposition temperature was slightly higher, but not enough to be significant.

We have investigated the effects of surface temperatures on films; at a temperature of 375°C, the film has a good absorption spectrum, and the X-ray diffraction pattern shows only the sphalerite phase. Unfortunately, the deposition efficiency decreases with increasing temperature.

Films were sprayed with varying copper content because Buldhaupt et al.[7] have found that an excess of copper at the interface is to be avoided in order to prevent diffusion of copper into CdS. They use a P+/P structure with additional copper in the P+ region. Our results are essentially in agreement with theirs as to resistance, as shown in Table 16. These films were about 0.5 μm thick and the resistivity of Sample 7-18A is calculated as 0.35 Ω-cm. The chemical analysis shows an excess of selenium and the expected change in copper content. We have used this concept to produce P+/P layers for device development.

We have now established that a Cu:In:Se ratio of 1:1:4 was correct for producing a film with an absorption spectrum and X-ray diffraction pattern that shows that the film was free of significant amounts of

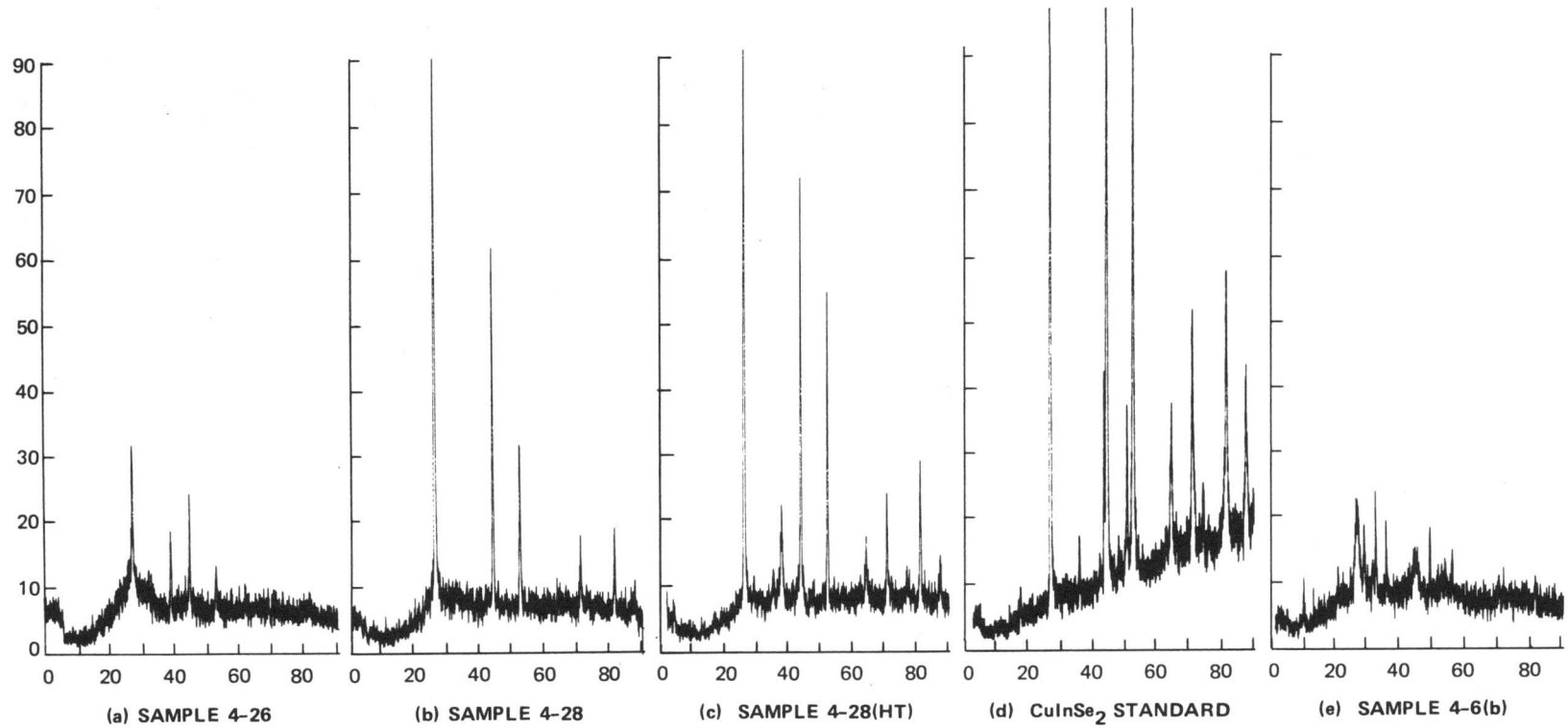

FIGURE 8 X-RAY DIFFRACTION PATTERNS OF $CuInSe_2$ FILMS

Table 16

$CuInSe_2$ FILMS WITH VARYING COPPER CONTENT

Sample Number	Cu:In:Se Ratio	Resistance ($\Omega/\square$)	Chemical XRF Analysis*
7-18A	1.1:1:4	7×10^3	$Cu_{0.97}InSe_{2.8}$
7-18C	1:1:4	2.5×10^5	$Cu_{0.92}InSe_{2.95}$
7-18B	0.9:1:4	8×10^7	$Cu_{0.85}InSe_{2.45}$

*X-ray fluorescence normalized to indium with Brown University standard.

other phases. We have also determined that a bath temperature of 375°C (corresponding to about 325°C surface temperature, according to Figure 1) produced a film with a good absorption spectrum and X-ray diffraction patterns showing only sphalerite lines. At surface temperatures of 180°C and 225°C, the films contain a second phase, which is probably $Cu_{2-x}Se$.

The as-sprayed films have always been of the sphalerite/crystal structure, which can be converted to chalcopyrite by heat treating.[8] We have found that the copper content of the solution from which a film was sprayed has a significant influence upon the phase transformation. Films prepared with a 0.9:1:4 and a 1:1:4 Cu:In:Se concentration ratios are not converted to the chalcopyrite by a 10-minute 600°C heat treatment in nitrogen, while a film sprayed from a 1.1:1:4 solution is. Loferski et al.[8] reported that a 15-hour, 500°C heat treatment in $CuInSe_2$ powder under vacuum produced the chalcopyrite.

The X-ray diffraction patterns are shown in Figure 9. We also have heat-treated the 1.1:1:4 film at 600°C, 500°C, and 400°C for 10 minutes; the resultant X-ray diffraction patterns are also shown in Figure 10. The arrows in Figures 9 and 10 indicate the location of the significant chalcopyrite lines (213/105, 211, 101),[8] confirming that the phase transformation takes place at lower temperatures than the 600°C of our earlier studies. We have also sprayed at an even higher copper content

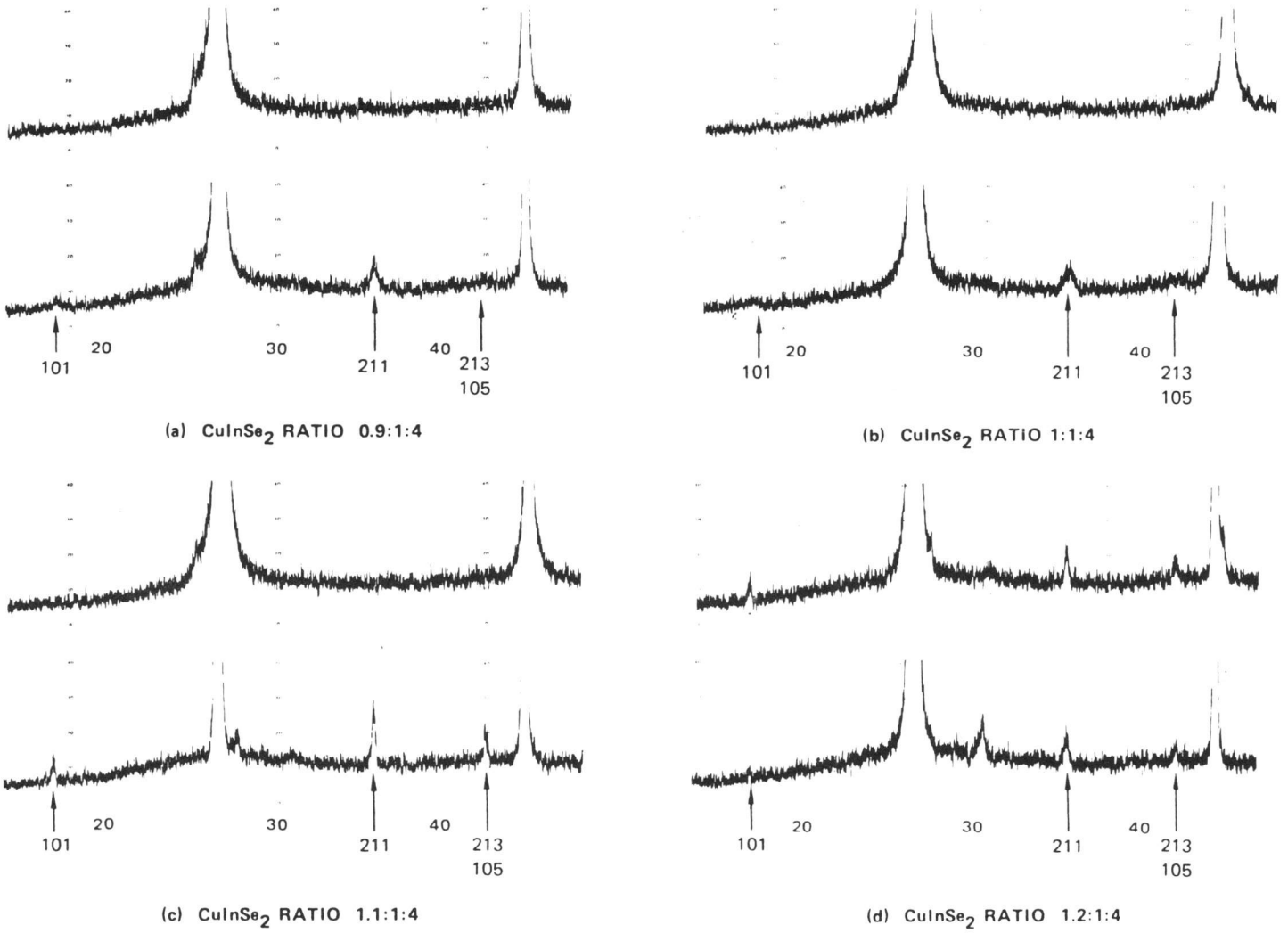

FIGURE 9 XRD SPECTRA OF $CuInSe_2$ FILMS SPRAYED WITH VARYING COPPER CONCENTRATIONS AND WITH AND WITHOUT HEAT TREATMENT

Lower trace in each pair heat treated at 600°C

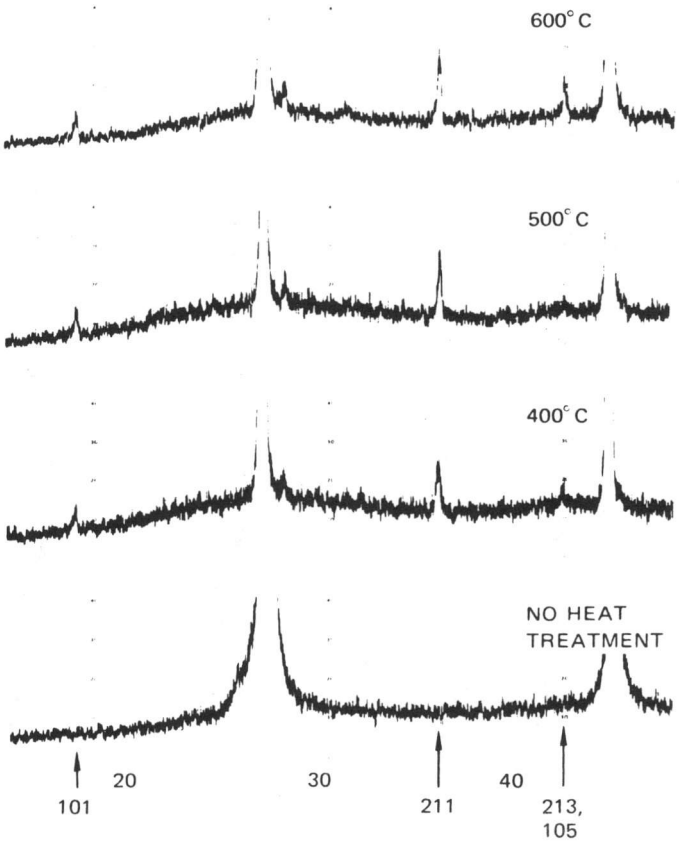

FIGURE 10 XRD SPECTRA OF 1.1:1:4 $CuInSe_2$ FILMS WITH VARYING HEAT TREATMENTS

All films from Sample 7-18-A

(viz., 1.2:1:4) and found that chalcopyrite lines appear in the as-sprayed film. However, the film converts to sphalerite on heat treatment. These diffraction patterns are also shown in Figure 10. We have not been able to determine the reason for this surprising result.

III STUDIES OF SINTERED LAYERS

The original paper on screen-printed and sintered photovoltaic devices by Nakayama et al.[9] specified a sintered CdS film of approximately 20 μm thickness with a CdTe heterojunction of about 10 μm thick. The films were prepared from powdered materials of approximately 2-μm particle diameter using $CdCl_2$ as the sintering flux in both cases. It is apparent from Nakayama's work that they used indium-doped CdTe in the beginning, probably from an indium-doped ground ingot. indium doped. The CdS layer was originally doped with $GaCl_2$. Our first experiments directed toward the preparation of controlled crystal size CdTe using techniques that had been developed for CdS[10] were relatively unsuccessful. The objective was to obtain very small starting crystals of CdTe, which were to be heated in a HCl/N_2 atmosphere at approximately 600°C. Our experience with a similar growth method for CdS had resulted in crystals of approximately 2 μm diameter, which were uniformly doped with chlorine; however, when we attempted a similar treatment of CdTe, we found that the growth rate of CdTe is much greater than that of CdS under similar circumstances and that the crystallites of CdTe could not be controlled in the size range below 10 μm. Consequently, the program for the growth of chlorine-doped CdTe crystals was discontinued and the following work with CdTe was done with commercially available 99.99-percent CdTe, which was ground in a mortar and pestle to produce crystal sizes less than 10 μm in diameter.

One basic problem in preparing sintered layers is the introduction of the flux. The sintering of cadmium chalcogenide films is based upon the use of a low melting, volatile material in which the chalcogenide is soluble. $CdCl_2$ is an ideal flux for CdS and CdTe. At the sintering temperature of 600 to 700°C, the CdS and CdTe are both soluble in the $CdCl_2$, and insufficient $CdCl_2$ is added to dissolve all of the CdS or CdTe that is present. The small amount that does dissolve acts as a

cement between individual grains when it reprecipitates epitaxially on them, building bridges between these grains, and forming a sintered mass. This is possible because of the relatively high vapor pressure of $CdCl_2$ of 10 mm at 656°C (melting point 568°C).

One practical difficulty in preparing a suspension from which films can be layered is the uniform distribution of $CdCl_2$. This problem has been solved by Nakayama and coworkers[9] by the use of a single solvent, propyleneglycol, as a suspension vehicle and as a solvent for $CdCl_2$. In preparing the suspension, the $CdCl_2$ is first dissolved in the appropriate quantity of propyleneglycol; then the CdS (or CdTe) is added accordingly. This suspension is then ground in a ball mill to produce a uniform mixture. This mixture is then applied to the surface, either the conductive-coated glass in the case of the CdS, or the presintered CdS layer in the case of the CdTe.

The Matsushita group[9] used a silk-screening process to apply their layers; however, we have found that it is more convenient to use a doctor blade machined from a steel bar of 6- x 6-mm cross section; two of the sections were machined on one surface to a height of approximately 40 μm and spaced about 2.5 cm apart. These projections are each about 4 mm wide; thus, when a film is applied to a glass substrate, the resultant film has two bare tracks approximately 2.5 cm apart and 4 mm wide. The glass substrate that is used in this project is Corning 7059 substrate glass. This is the same glass that is used for the spray pyrolysis substrate. Throughout the program we have experimented with both conductive coated glass and glass that has no conductive coating on it, as suggested by Nakayama[11] in a recent publication.

After the film has been layered onto the glass, it is dried overnight at room temperature and introduced into a 57-mm-diameter tube furnace, which is flushed with nitrogen for 30 minutes while the furnace is being heated to the sintering temperature. Then the layer on its Pyrex substrate supported on a flat quartz plate is put into the hot zone of the furnace, where it remains for the specified period of time depending upon the desired conditions; the substrate is then extracted from the

hot furnace into the cold zone, where it is allowed to cool in flowing nitrogen to well below 300°C before being removed from the tube and its inert atmosphere. The resultant layers, which are composed of sintered grains of cadmium chalcogenide compound, are quite porous. We have had considerable success in reducing the porosity of the CdTe films to approximately 80 percent of theoretical density. However, the success with the CdS has not been comparable. Our best films are approximately 50 percent of theoretical density. We attribute this fact to poor packing during the layering process, as well as the space remaining after the $CdCl_2$ and propyleneglycol have evaporated. We have attempted to increase the packing density of these films by centrifuging. The layered films were placed in a large centrifuge of about 2-foot diameter and spun at 1000 to 1500 rpm, but the resultant films did not seem to have an improved density. After a number of experiments with doping with gallium and hydrogen firing, as reported by Zanio,[12] we investigated a process reported by McDonald and Goodman,[13] who use a much higher quantity of flux than was reported by Nakayama.[9] Our first experiments with high flux levels were successful and we continued this along with the introduction of $CdSO_4$, as recommended by a Matsumoto et al.[14]

Table 17 summarizes the results of a series of experiments in which the flux level was varied and the layers heat-treated in nitrogen and nitrogen containing cadmium vapor at 630°C for 60 minutes. The addition of cadmium vapor to the sintering atmosphere was suggested by Matsumoto et al.[14] and is accomplished by incorporating a cadmium source in a 400°C zone in the tube furnace.

Figures 11 and 12 are scanning electron microscopy (SEM) photographs of the same layers, and show that the presence of increasing $CdCl_2$ results in considerable grain growth and obvious bridging between grains. The effect of the cadmium is even more dramatic, but the reduction of resistance upon the addition of cadmium is not as great as the appearance of the layer would lead one to expect.

Table 17

INFLUENCE OF FLUX CONCENTRATION ON RESISTANCE*

Sample Number	$CdCl_2$ (%/wt)	Resistance (Ω/□)	Thickness (μm)	Resistivity (Ω•cm)
1-35	53	3200	10	3.2
1-35-Cd	53	1700	15	2.5
5-44-A	26	1500	25	3.7
5-44-A-Cd	26	500	28	1.4
5-44-B-Cd	14	500	46	2.3
5-1	6.8	7000	20	14
5-1-Cd	6.8	4500	20	9

* All samples fired at 630°C for 30 minutes in nitrogen or N_2-Cd atmosphere, as indicated.

Subsequent experiments with the addition of $CdSO_4$ to introduce sulfur vacancies [as reported by Matsumoto et al.[14]] had a marginal effect on resistance at high $CdCl_2$ levels. Doping of the CdS layer with $GaCl_2$ also gave varied results, with one sample having a low resistance for a low $CdCl_2$ flux level. In both cases, the results were inconclusive, but at least encouraging. $CdSO_4$ addition has been used in layers that were used for device preparation.

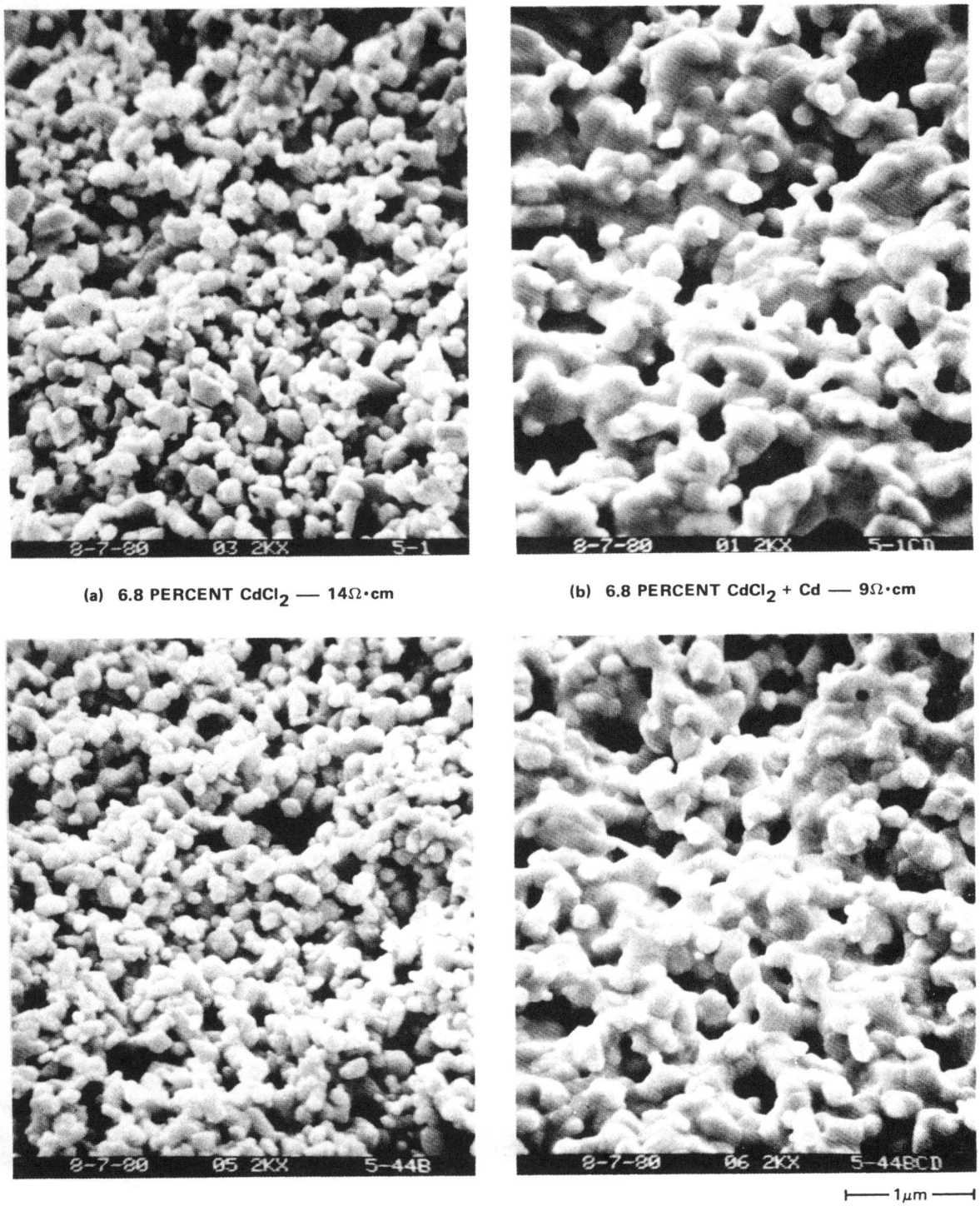

(a) 6.8 PERCENT $CdCl_2$ — 14Ω·cm

(b) 6.8 PERCENT $CdCl_2$ + Cd — 9Ω·cm

(c) 14 PERCENT $CdCl_2$

(d) 14 PERCENT $CdCl_2$ + Cd — 2.3Ω·cm

FIGURE 11 SCANNING ELECTRON MICROGRAPHS OF SINTERED FILMS AT 2000X

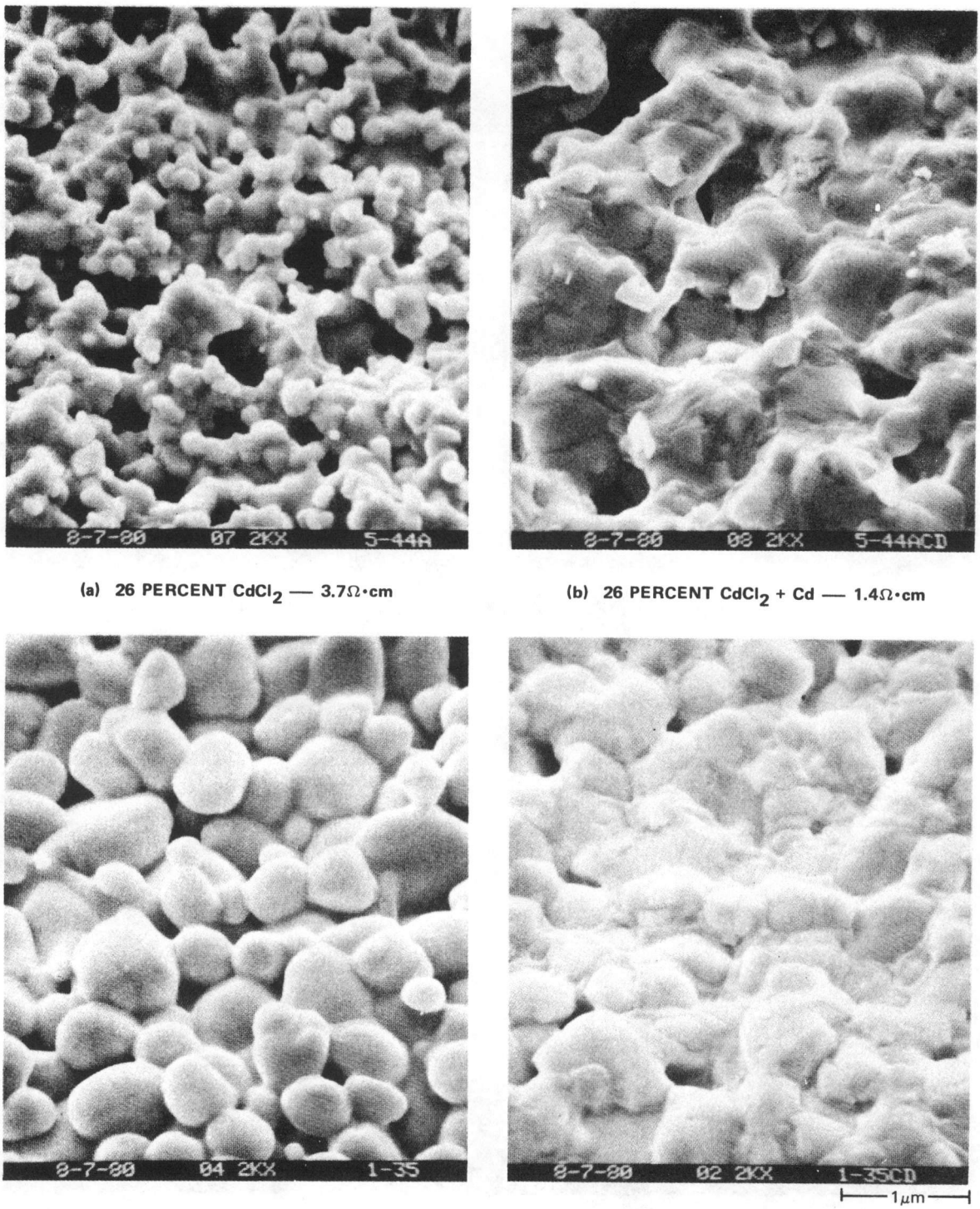

(a) 26 PERCENT $CdCl_2$ — 3.7Ω•cm

(b) 26 PERCENT $CdCl_2$ + Cd — 1.4Ω•cm

(c) 53 PERCENT $CdCl_2$ — 3.2Ω•cm

(d) 53 PERCENT $CdCl_2$ + Cd — 2.5Ω•cm

FIGURE 12 SCANNING ELECTRON MICROGRAPHS OF SINTERED FILMS AT 2000X, INCREASING $CdCl_2$

IV WORK WITH SPRAYED CELLS

The first device was a glass/SnO_2(Sb)/CdS/$CuInS_2$/Au heterojunction. Because the lattice match between CdS and $CuInS_2$ is poor, good response was not expected. Experimentally, the serious problem arose from the differential thermal expansion of the two layers, resulting in cracking of the layers. An array of 0.02 cm^2 gold dots was deposited by vacuum evaporation. One dot happened to reside entirely within an island surrounded by the cracking pattern and the photoresponse could be measured. Figure 13 is the oscilloscope trace of the I-V curve under 150 mW/cm^2 tungsten (ELH) illumination.

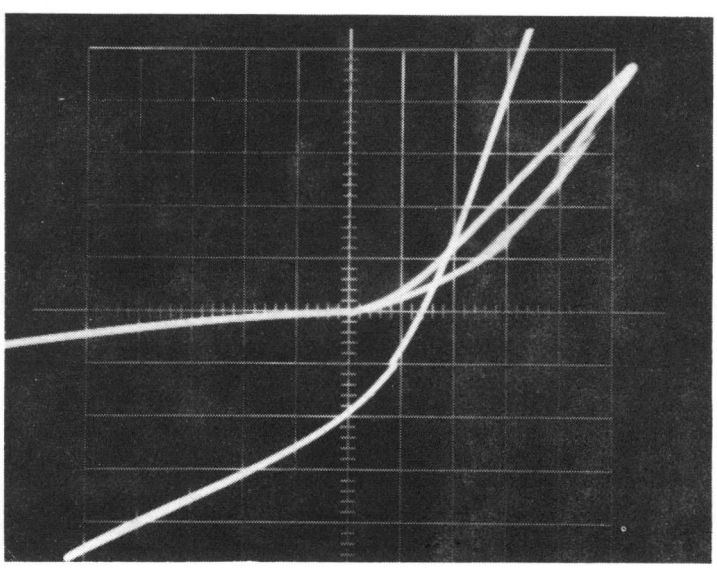

FIGURE 13 PHOTORESPONSE OF SPRAYED CELL

Structure is glass/SnO_2(Sb)/n-CdS/p-$CuInS_2$/gold.
P_o = 150 mW/cm^2, A = 0.02 cm^2, V_{oc} 0.28V, I_{sc} 0.095 mA

The sprayed device can be in two configurations:

- Front wall (glass/Au grid/$CuInSe_2$/CdS/Al)
- Back wall (glass/ITO/CdS/$CuInSe_2$/Au).

Our original proposal specified the front-wall configuration to avoid the optical loss resulting from absorption by the CdS. The ideal thickness of the $CuInSe_2$ layer appears to be a difficult problem, and we have been able to produce only two devices that exhibited a photovoltaic response. We now believe that if the thickness of the $CuInSe_2$ layer is reduced to the level where the absorption occurs in the high field region, it will be less than 0.5 μm thick and the sheet resistance will be too high for efficient charge collection. The back-wall cell has the disadvantage that the sunlight enters through the CdS layer, where losses resulting from absorption outside the field region are significant. This disadvantage is outweighed by the advantage that the remaining light is absorbed in the correct region. Not only have our results been better in this configuration, but the successful devices developed by Buldhaupt et al.[7] were also of the back-wall configuration. They have also used a N+,N/P,P+ configuration through control of the Cd:S and Cu:In:Se ratios.

It is expected that a similar structure will be useful in spray pyrolyzed devices. The conductive form of CdS is sprayed from a sulfur-deficient solution (see Section II-C). The conductivity is attributed to the sulfur vacancies, which would also contribute to enhanced copper diffusion from the $CuInSe_2$ into the CdS during heat treatment, producing an insulating region. To minimize the sulfur vacancy content near the interface, the last part of the deposition is made with an increased thiourea concentration. This region will be of higher resistivity, but will be thin and may not introduce excessive series resistance.

We know that increased copper content results in lower resistivity in the p-region. Also, phase transformation at 400°C is possible if a 1.1:1.4 Cu:In:Se solution composition is used. The excess copper can

readily diffuse into the CdS, so it may be advisable to lower the copper content of the solution during the deposition of the first 20 percent of the $CuInSe_2$ layer.

Table 18 summarizes the results for a number of recent devices. It is apparent that a temperature above 260°C for the $CuInSe_2$ spray is important. This is not desirable from the efficiency of deposition standpoint, but appears to be important. These results are not reproducible enough to determine whether the layered structure is advantageous.

Table 18 includes Sample 7-42-S, in which an alloy $Zn_{0.26}Cd_{0.84}S$ was used in place of the CdS layer. The Wurtzite CdS lattice constant is 5.850 angstroms, that for chalcopyrite $CuInSe_2$ is 5.782 angstroms, for ZnS it is 5.410 angstroms, and 5.78 for $Zn_{0.16}Cd_{0.84}S$. This alloy has a near-perfect match for $CuInSe_2$ and should have fewer interface states. There is also an electron affinity advantage; however, the resistivity of $Zn_xCd_{(1-x)}S$ alloys is usually greater than that of CdS.[15] The result shown in Table 18 for the alloy is not significantly different from zinc-free cells.

Further work on the alloy will be required after other more significant problems that limit efficiency have been solved.

Table 18

BACK-WALL CELL
Glass/ITO/CdS/Cu_2InSe_2/Al(Ag paint)

Sample	ITO Resistance (Ω/□)	Cd:S Ratio	$CdCl_2$ (m moles)	Surface Temperature (°C)	Cu:In:Se_2 Ratio	Temperature (°C)	Diode	V_{oc} (V)	J_{sc}* (mA/cm^2)
7-11-A	500	1:0.9	0.5	325	1:1:4	260	No	–	–
7-12-5	500	1:0.9	1.0	325	1:1:4	260	Yes	–	–
7-25	200	1:0.9 1:5	1.25	325	0.9:1:4 1.1:1:4	325	Yes	0.2	12
7-35	1000	1:0.9	1.5	325	1.1:1:4	325	Yes	0.28	1.6
7-38	1000	1:0.9 1:2	1.5	325	0.9:1:4 1.1:1:4	325	Yes	0.12	6.8
7-40-B	5000	1:0.9	2.0	325	1.1:1:4	325	Yes	0.2	7.2
7-42-5†	1000	1:1	0.5	325	1.1:1:4	325	Yes	0.25	7.2

*For a 0.25 cm^2 area, 100 mw/cm^2.

†Zinc alloy $Zn_{0.16}Cd_{0.84}S$.

V SINTERED CELLS

A. Background

The objective of the sintered cell program is to evaluate the process for the preparation of a CdS/CdTe cell by screen printing and sintering as reported by Nakayama et al.[9] In our work, we have used doctor blading rather than screen printing as the layer application method because it is equally effective and avoids the rheology problems associated with screen printing.

Since this original paper the Matsushita group has published a number of others,[11,16-19] which have clarified their original publication.[9] The relevant papers are summarized in Table 19.

Originally, Makayama and coworkers[9] were of the opinion that the device was actually a homojunction:

glass/ITO/CdS/p-CdTe/n-CdTe/Cu_2Te/Ag.

However, later[11] they decided that the CdTe could be entirely converted to p-type and the heterojunction was significant. They have also[11] eliminated the ITO layer by reducing the resistance of the CdS (see Section III). This avoids the possibility of shorting the junction through the porous layer, but increases the series resistance.

Table 19 summarizes the significant references, including a summary of a trip report by M.B. Prince of DOE,[19] and the results of the SRI work to date.

The most important questions in this program are, where is the junction and what is its nature? The classical wet CuCl process of

Table 19

SUMMARY OF CELLS REPORTED BY MATSUSHITA AND SRI
All devices on ITO-coted glass

Cell Characteristics	Reference						
	Nakayama [9]	Ikegami [16]	Nakano [17]	Nakayama [18]	Prince [19]	SRI	Nakayama [11]
CdS Layer							
Composition	CdS + ?	CdS + (0.3-1%)$GaCl_2$ + (3-5%) $CdCl_2$ + Propylene glycol	CdS + $GaCl_2$ + $CdCl_2$	Unknown	CdS + (0.2-1%)$GaCl_2$ + (3-5%)$CdCl_2$ + Propylene glycol	CdS + $GaCl_3$ + $CdCl_2$ + N_2=HCl	CdS + (0.3%)$GaCl_2$ (5%)$CdCl_2$ Propylene glycol
Thickness (μm)	20*	25	Unknown	Unknown	25	50	20 ∿ 25 μm
Heat treatment	?	630°C in N_2	630°C in N_2	630°C in N_2	Dry at 120°C; 650°C in N_2	650°C in N_2	630°C in N_2 for 20 min
CdTe Layer							
Composition	n-CdTe(In) + $CdCl_2$	CdTe + $CdCl_2$ + <1% Propylene glycol	Unknown	Cd + Te "No $CdCl_2$"	CdTe (pure) + <1% $CdCl_2$	CdTe (pure) + CdTe(In) + <1% $CdCl_2$	CdTe (pure) <1% $CdCl_2$
Thickness (μm)	10+	15	Unknown	Unknown	15	20	
Heat treatment	500-800°C in N_2	Unknown	Unknown	600°C in N_2 for 60 min	720°C	720°C	720°C in N_2 for 60 min
Contact							
p-Region	Cu_2S (wet)	Carbon	Unknown	Unknown	Carbon (Cu)	CuCl and Carbon	CuCl and Carbon
p-Contract	Ag paint	Ag paint	Unknown	Unknown	Ag paint	Ag paint	Carbon (Cu)
n-Contact	In-Ga	In-Ga	In-Ag paint	Unknown	In-Ag paint	In-Ag paint	In-Ga
Heat treatment	200°C for 10 min	300°C in N_2	Unknown	Unknown	300°C	300°C	300°C for 30 min
Performance							
V_{oc} (V)	0.68	Unknown	0.64	0.68	3.43‡	0.41	0.73
I_{sc} (mA)	31	Unknown	10.8	12.7	711‡	0.74	11.4
FF (%)	Unknown	Unknown	Unknown	38	50.8‡	12	51
AM1 Efficiency (%)	8.1	8.1	4.3	4.7	5.5§	0.2	6.3

*Bulk resistivity was 0.2 Ω-cm.

+Bulk resistivity was 0.1 to 10 Ω-cm.

‡For five-cell array.

§For active area; overall module efficiency was 3%.

Cu_2Te formation was used at first.[9] Later papers[11,16-19] all refer to a carbon electrode. Prince[17] reports that copper impurities are added to the carbon paste.

The contacts have also varied. Nakayama[9] used a silver paint on the p-type layer and an In-Ga electrode on the CdS. Ikegame[16] indicates the same electrode. The subject of Nakano's paper[17] is a screen-printable electrode made by adding indium powder to a commercial silver paint; this electrode was included in the presentation reported by Prince.[19]

The CdS layer preparation process is the same in all reports with the exception of cadmium vapor in the sintering atmosphere.[14] $CdCl_2$ is used as a flux, and the three references that report on gallium doping refer to $GaCl_2$ as the source of gallium. The boiling points of $GaCl_2$ is shown in the CRC Handbook[20] as being higher than that of $GaCl_3$: 535°C against 201°C. Because Ga III functions as a donor in CdS, oxidation must occur at some point in the process. We assume that the Ga II compound is used because of its low volatility.

The CdTe layer was made from indium-doped n-type CdTe. Nakayama and coworkers[9] report that the sintered CdTe layer is 10^{-1} to 10Ω-cm and that the resistivity of the bulk that was used to make the paste was 0.2 Ω-cm. Therefore, they must have pulverized a larger crystal to produce their powder. Prince[19] reported that Matsushita used 99.99-percent CdTe and does not mention indium doping. Later Nakayama[11] stated that they were no longer using indium doping because they wanted the CdS/CdTe heterojunction. Nakano[11] reported that a borosilicate substrate was used, Nakayama[17] mentioned a high-quality glass, and Prince[19] said that one remaining problem is a low-cost glass substrate. The softening point of borosilicate glass (Pyrex, Corning No. 7740) is 821°C, and that of PPG float glass is 725°C. The highest processing temperature in Table 18 is 720°C; however, 600°C is the maximum temperature in the new Cd + Te →CdTe reported by Nakayama.[18] Our experience[21] in processing photoconductors on glass substrates for electrophotography has been that soft glass can be routinely processed at 550°C if the rate of

temperature rise and fall is compatible with the thermal shock of the glass. Electrophotographic CdS layers, which have a bulk resistivity of 10^{12} Ω-cm or better for the photoconductor plus binder, are so heavily compensated by copper that they are unaffected by impurities emanating from the glass substrate. If soda lime substrates are processed at 600°C, the softening and deformation of the glass is apparent despite the 725°C rating, and diffusion of impurities (such as sodium) into the CdS is probable.

Our experimental program has investigated a number of variations in the form of the sintered device. The original proposal envisioned a device in which the spray-pyrolyzed CdS layer would be substituted for the sintered CdS layer. The rationale for this design was that a semi-transparent sprayed film of a few micrometers thickness would constitute a better window than would 20 or 25 μm of sintered powder. This proved unworkable because the sintering CdTe layer or its flux reacted with the CdS layer except in the middle of broad areas. It appeared that the attack occurred from the edges of the delineated CdTe layer, and it may be that the actual structure is:

$$\text{glass/In-Ga/ITO/n-CdS/n-CdS}_x\text{Te}_{(1-x)}\text{/n-CdTe/p-CdTe/carbon/silver.}$$

If this is in fact true of the spray-deposited surface, then it must also enter into the sintered device, although probably in a still more complex geometry.

Our proposal also contemplated producing n-type CdTe powder by doping 99.999-percent CdTe with chlorine and indium under conditions that, from our experience with CdS, were expected to recrystallize the CdTe and result in a fairly narrow range of crystal sizes (see Section III). The advantages of this approach were that, by starting with micrometer-sized particles and growing them in an atmosphere containing the dopants, the resulting regrown crystals would have uniform dopant distributions. If the growth process could be controlled so as to produce crystals of 5 to 10 diameter, it would not be necessary to grind them to a reduced crystal size. Grinding is a damaging process, in that it

introduces impurities from the grinding media and in that it can damage the crystal lattice. As reported in Section III, we have been unable to find a set of conditions under which we can control the size distribution of CdTe. We have proceeded with chlorine- or indium/chlorine-doped CdTe that was ground after doping in a tube furnace. We have found no significant difference in the chlorine- or chlorine/indium-doped CdTe as far as the resistance of the layer is concerned. Recent layers have been made with undoped 99.999 percent CdTe (Gallard Schlessinger). It is difficult to measure resistivity of a sintered layer with precision because of the problem of applying and defining the contact. We did measure the resistance between a pair of silver paint dots and calculated a bulk resistivity of 0.1 to 0.2 Ω-cm. Normally, CdTe layers are prepared on CdS layers, and we measure the resistivity with a pair of conducting rubber probes that have dimensions and spacings appropriate for an Ω/□ measurement. Because the resistivity of the CdTe is usually lower than that of the CdS, we believe that this is a reasonable measurement. At this point, our primary interest is in the junction and how it is formed; hence, our principal efforts are directed toward these questions.

In our first efforts, we succeeded in producing heterojunctions on sprayed CdS as described above, and on sintered CdS layers that were doped with gallium and chlorine. We also tried (without success) a modified wet CuCl process, and a carbon paste mixed with CuCl solution. We were not successful in producing a photosensitive device, although a diode characteristic was observed in the one in which an undoped carbon electrode was applied. Because none of these approaches was successful, we attempted to restrict the junction by partially filling the porous structure with a solvent. The concept was to fill the porous sintered mass with a fluid that will prevent penetration by the suspension of carbon and dopant films; the hope was that the resulting junction would be in the upper portion of the CdTe layer.

In the first experiment (Sample 3-22), we used chloroform to define the junction because chloroform is heavier than water (which is the

vehicle for Graphilm, a carbon suspension marketed by Asbury Graphite films, Inc.). Copper, in the form of 1 ml of 0.625 mol CuCl, was added to 10 ml of graphite and painted on 1-cm^2 areas delineated in the CdTe layers. The substrate was SnO_2-coated glass with a sintered gallium-doped CdS layer and an indium-doped CdTe layer. The CdTe layer was formed at 720°C for 30 minutes in nitrogen. The Graphilm was painted on the 1-cm^2 areas with care to avoid going outside the CdTe and thereby shorting the junction. The contacts were baked at 300°C in nitrogen for 30 minutes. The contact to the CdS was silver-indium paint; silver paint was used for the contact to the graphite.[16] This device was tested and found to be ohmic.

B. Microscopic Studies

The device was broken and the edge examined under the microscope and with the scanning electron microscope. Figure 14 is a photomicrograph taken at 170X; the various layers are indicated in the figure.

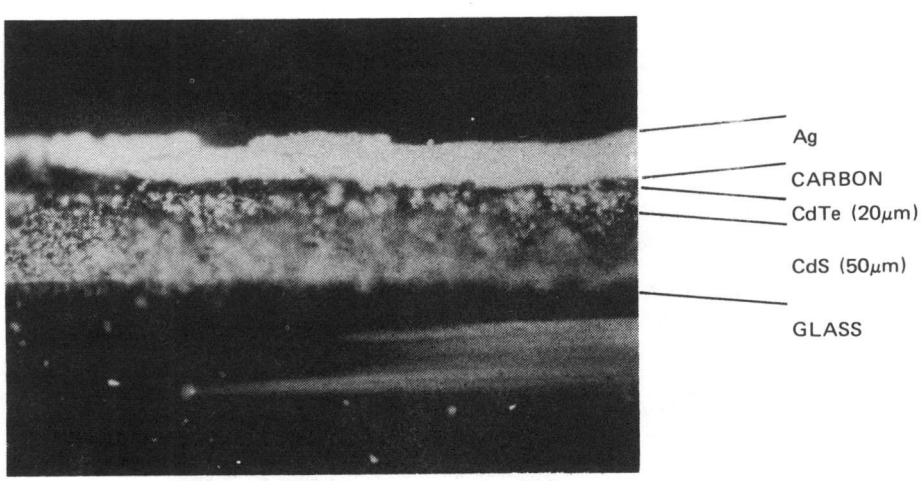

FIGURE 14 PHOTOMICROGRAPH OF SINTERED DEVICE 3-32 AT 170X

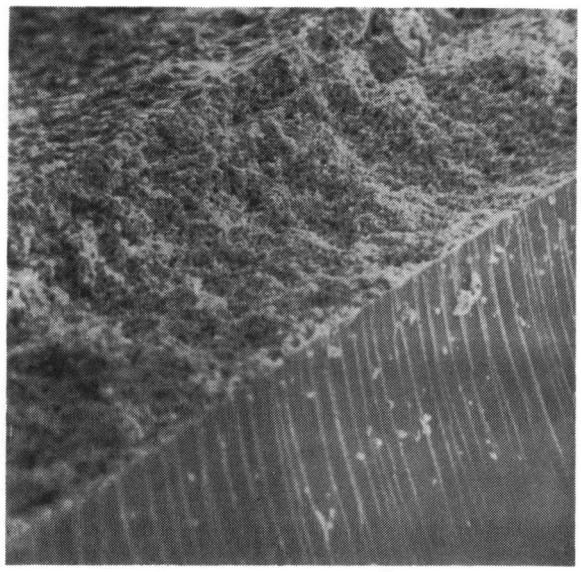

(a) BROKEN EDGE AT 200X SHOWING STRUCTURE

(b) SAME AREA AS (a), BUT AT 500X

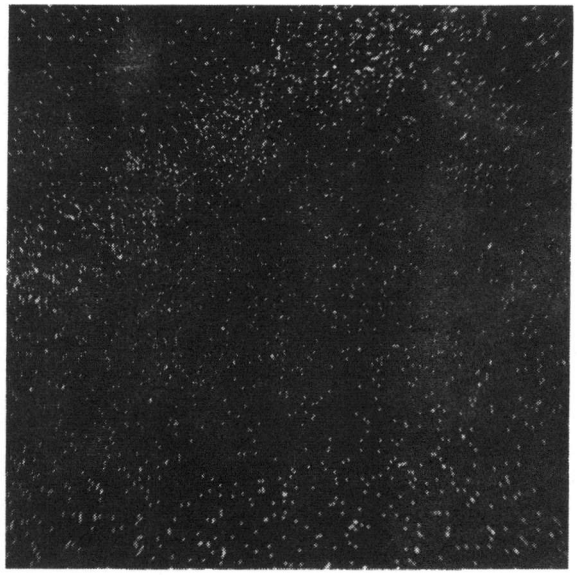

(c) TELLURIUM DISTRIBUTION AT 500X

FIGURE 15 SCANNING ELECTRON MICROGRAPHS OF SINTERED DEVICE 3-32

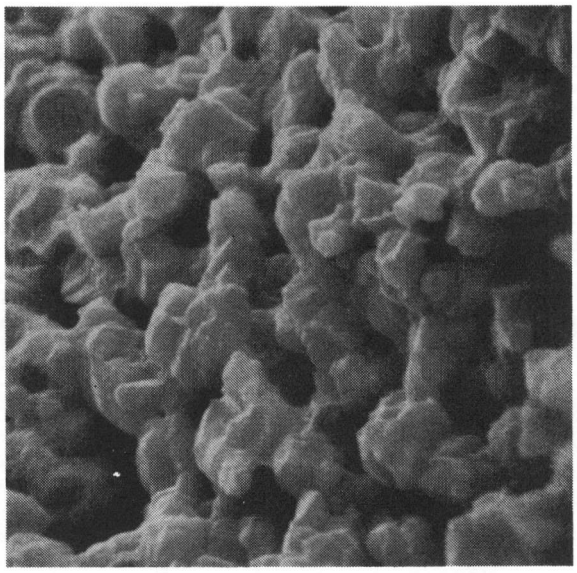

(d) CdS LAYER AT 500X

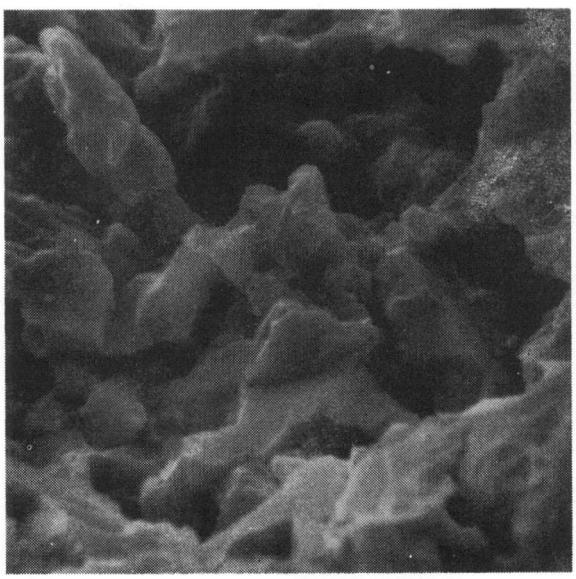

(e) CdTe LAYER AT 500X

FIGURE 15 SCANNING ELECTRON MICROGRAPHS OF SINTERED DEVICE 3-32 (Concluded)

Figure 15 are SEM representations of the same sample. Figure 15(a) is a 200X view of the broken edge, showing the glass, the sintered CdS, the sintered CdTe, and the carbon. This area did not have a silver contact. Figure 15(b) shows that a distinct difference is still visible at 500X. Figure 15(c) is the same area viewed with the x-ray fluorescence system and using a window adjusted for tellurium radiation; the CdTe layer is clearly defined. The signal outside this area could as easily be noise as tellurium that has diffused into the other layers, as discussed earlier.

Figures 15(d) and 15(e) are 500X views of the CdS and CdTe layers, respectively, showing the good sintering that occurred during the processing and the resulting porosity. These layers appear to be less dense than the 80 percent of theoretical that is reported in Section III, although the preparation was essentially the same.

In Sample 3-29, the glass substrate had a chromium grid of 0.25-mm lines on 2.5-mm centers, and SnO_2(Sb) had been spray deposited over this grid. The sheet resistance was about 300 Ω/□. The CdS layer was prepared from a suspension of 20 g of 99.999-percent CdS, 0.13 g $GaCl_3$, and 0.40 g $CdCl_2 \cdot 2.5\ H_2O$ in 15 ml propylene glycol. After drying at 120°C in nitrogen for 60 minutes and sintering at 650°C for 60 minutes in nitrogen, the sheet resistivity of the sintered layer was 10 to 100 Ω-cm. The CdTe layer was prepared from a mixture of 10 g of CdTe with 0.075 g $CdCl_2 \cdot 2.5\ H_2O$ and 6 ml of propylene glycol. The suspension was applied with a doctor blade with a 0.125-mm gap, dried at room temperature for 72 hours and at 120°C for 24 hours, then fired at 650°C for 25 minutes. The resistivity was then approximately 1 Ω-cm.

The CdTe film had been patterned into seven 1-cm^2 squares before the heat treatment. The areas between these squares where the CdS was exposed were first saturated with glycerine by impregnation to prevent the capillary diffusion of the contact material around the CdTe. Three pretreatment conditions were applied to the CdTe areas in an attempt to limit the location of the junction. These pretreatments and the three levels of contact dopant are summarized in Table 20. The sample was

heat treated at 300°C in nitrogen for 20 minutes. Contacts were evaporated indium on the CdS and evaporated gold on the CdTe/carbon. Silver paint was added to the gold because of the fragile nature of the sintered material. All areas were ohmic and none exhibited a diode characteristic. Scribing the 1-cm^2 areas into smaller squares in an attempt to avoid any area in which there might be shorting around a junction did not result in any improvement.

Table 20

SUMMARY OF PREPARATION OF SAMPLE 3-29

Area	Pretreatment	Carbon Suspension
1a	None	10 ml Graphilm, 0.5 ml 3.1 molar CuCl in HCl, 0.05 g tellurium powder; water added until fluid
1b	None	10 ml Graphilm, 5 ml 3.1 molar CuCl in HCl, 0.05 g tellurium powder; water added until fluid
2a	Glycerine	10 ml Graphilm, 0.5 ml 3.1 molar CuCl in HCl, 0.05 g tellurium powder; water added until fluid
2b	Glycerine	10 ml Graphilm, 5 ml 3.1 molar CuCl in HCl, 0.05 g tellurium powder; water added until fluid
3a	Isopar M	10 ml Graphilm, 0.5 ml 3.1 molar CuCl in HCl, 0.05 g tellurium powder; water added until fluid
3b	Isopar M	10 ml Graphilm, 5 ml 3.1 molar CuCl in HCl, 0.05 g tellurium powder; water added until fluid
3c	Isopar M	10 ml Graphilm, 0.5 ml 3.1 molar CuCl in HCl

*Pretreatment consisted of saturating the porous CdTe layer with glycerine or Isopar M [kersoene hydrocarbon, Exxon trademark], then blotting the surface dry and leaving the bulk saturated.

Despite the fact that a spray-pyrolyzed CdS layer is heavily attacked by the CdTe layer-formation process, our modest success in reducing the resistivity of spray-deposited CdS by hydrogen firing led us to attempt to form a junction on a particularly heavy spray-pyrolyzed CdS deposit that had been heat treated for 35 minutes at 400°C in H_2. A CdTe layer from the same source as the preceding sample was applied, dried, and heat-treated in nitrogen at 650°C for 25 minutes. A large

section of the CdTe layer vaporized or had reacted (alloyed) with the CdS. The area where the CdTe remained covered about half of the total substrate. Two small areas were coated with Graphilm and two with a mixture of 10 ml Graphilm and 0.5 ml 3 molar CuCl. After drying overnight, the device was fired at 300°C in nitrogen for 20 minutes. Silver and silver-indium contacts were applied immediately upon removal of the sample from the nitrogen atmosphere. Copper wire leads were attached with the paint, and the sample heated to 180°C in nitrogen to set the contact. The whole area was immediately sealed with Q-dope as an encapsulant. Tests indicate that all four areas were ohmic. This was designated Sample 3-31. The resistivity of the CdTe layer after device processing was 1 to 10 Ω-cm, assuming that the measured resistivity was unaffected by the higher resistivity CdS (10 to 100 Ω-cm).

We also repeated the latest Nakayama et al.[1] method restricting (for the present) our acceptor to wet-process ion exchange from CuCl, and we produced our first photovoltaic devices (Sample 5-7-C) with a maximum photoresponse of 0.38 V dc and I_{sc} of 20 μA under illumination of 75 mW/cm^2. This device was prepared on a SnO_2(Sb) conductive layer having 150 Ω/□ resistance. The mix contained 20 g CdS, 1.8 G $CdCl_2 \cdot 2.5 H_2O$, 0.4 g $CdSO_4 \cdot 8 H_2O$, and 18 ml propylene glycol. The CdS layer was heat treated at 630°C in N_2. An indium-doped CdTe layer containing 5 g CdTe 0.05 g $InCl_3$, 0.04 g $CdCl_2 \cdot 2.5H_2O$ in 3 ml propylene glycol was applied and, after drying, fired at 720°C for one hour in N_2. Silver-indium paint was applied to the CdS contact areas, which were then masked with a methacrylate paint. The device was dipped into CuCl solution at 75°C under N_2 for 10 seconds. The film was then dried, and heated for 10 minutes at 200°C. Silver paint dots were applied to the CdTe areas, and methacrylate applied as a sealant.

A second device (5-7-A) was prepared on a borosilicate glass substrate without a conductive coating. The $CdSO_4$ was produced by adding

H_2SO_4 to the $CdCl_2$ and heating it to drive off HCl; the indium doping level was 0.1 percent of the CdTe. The response of this cell was V_{oc} of 0.6 V and 60 μA I_{sc}.

Figures 16 and 17 show SEM photomicrographs of the two cells and the surface of the CdS layers of Samples 5-7 A and 5-7-C. The fact that Sample 5-7-C is more porous than 5-7-A may account for its lower photosensitivity. The CdS suspension Sample 5-7-C with the addition of $CdSO_4 \cdot 8\ H_2O$ was more viscous and did not form a layer as smoothly as did Sample 5-7-A. The increased indium content and lack of a transparent conductive layer in Sample 5-7-A are also important factors.

These results were encouraging in that they represented our first successful junctions. There were several variables to be studied: $CdSO_4$ and cadmium vapor in CdS formation, doping of the CdS, conditions of the Cu_2Te formation, and heat treatment times and temperatures. Given this many variables, considerable improvement in photoresponse can be expected.

We have produced a number of devices on CdS layers that were sintered in nitrogen and in nitrogen-cadmium atmospheres. The preparation and properties of these devices are listed in Table 21. Some devices were doped with $CdSO_4$ and $GaCl_2$ as discussed in Section III. The increase in photoresponse in the most recent samples (7-19-A, -B, and -C) could be influenced by improvements in the processing in CuCl solution, and our technique did improve with time. The CdTe layers were divided into 1-cm^2 squares before the sintering step. Before the copper dip, the CdS areas and the edges of the CdTe islands were masked with methacrylate resin. After the Cu_2Te had been formed and the 200°C heat treatment completed, contacts of silver-indium paint were applied as 2- to 3-mm dots, four or five dots to the 1-cm^2 area. The measurements in Table 19 are for the best of these dots. In the case of Sample 7-19-B, all of the dots in the 1-cm^2 areas were connected after measurement; surprisingly, the short circuit current remained nearly the same,

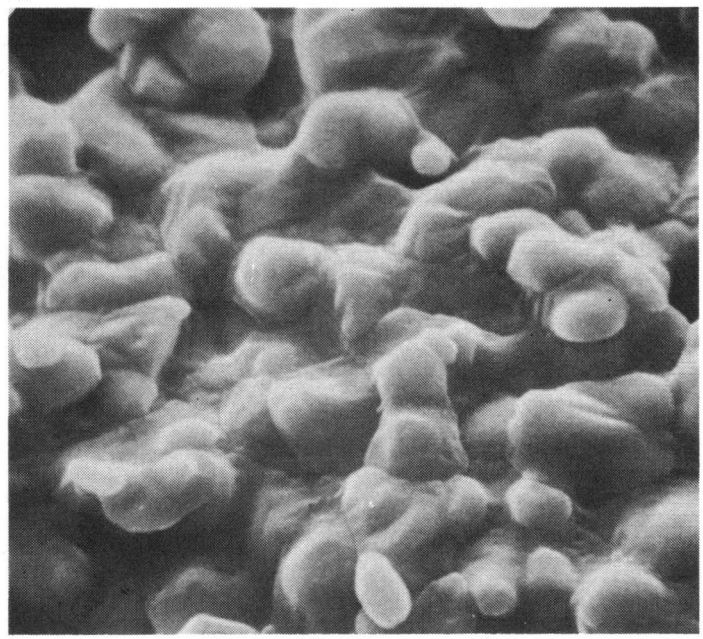

(a) TOP VIEW

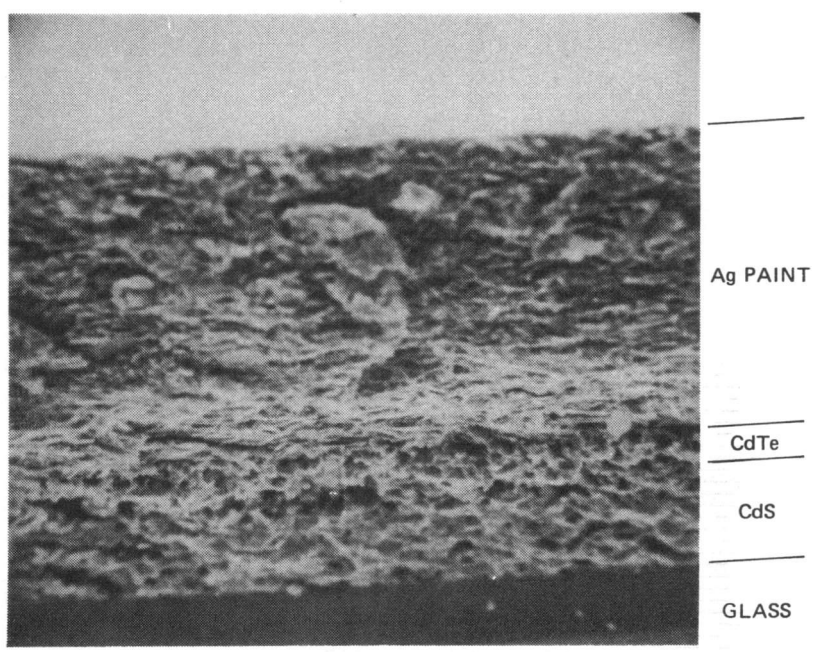

(b) CROSS SECTION

FIGURE 16 SCANNING ELECTRON MICROGRAPHS OF DEVICE 5-7(a)

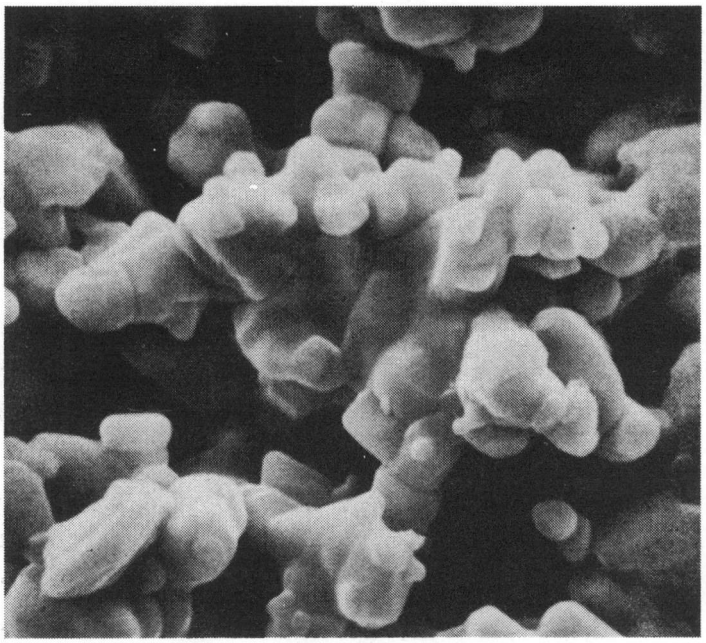

(a) TOP VIEW

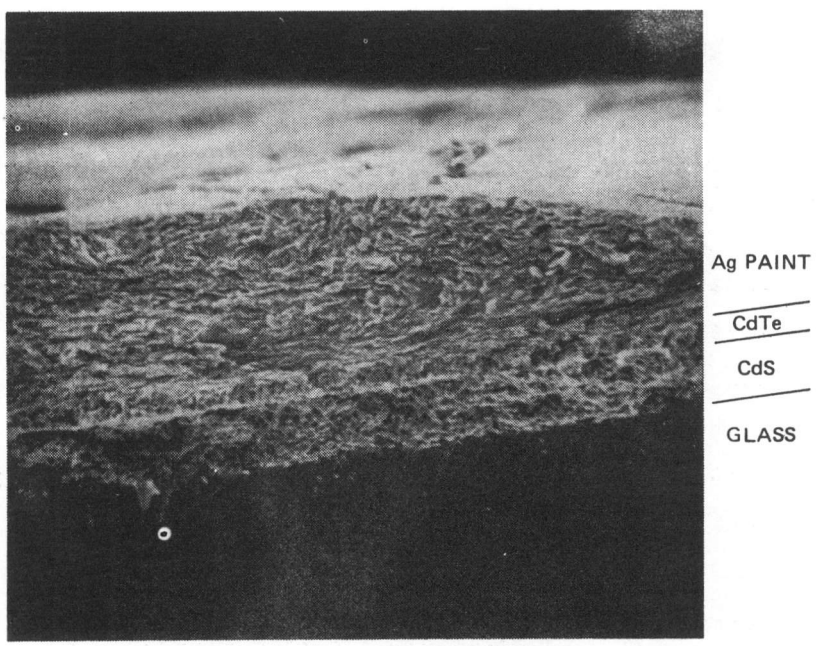

(b) CROSS SECTION

FIGURE 17 SCANNING ELECTRON MICROGRAPHS OF DEVICE 5-7(c)

Table 21

SINTERED DEVICES

Sample Number	CdS Dopant	Atmosphere	Thickness (Mm)	Resistivity (Ω/cm)	V_{oc} (v)	I_{sc_2} (A/cm^2)
5-46-A	None	N_2-Cd	30	60	0.50	3.7×10^{5}
5-47-B	$CdSO_4$	N_2-Cd	45	18	0.3	1.2×10^{-5}
5-46-B	None	N_2	30	--	0.2	1.4×10^{-5}
5-46-C*	$CdSO_4$	N_2	27	32	0.38	1.9×10^{-5}
5-47-C	$CdSO_4$	N_2-Cd	--	--	0.2	2×10^{-5}
5-47-A	$CdSO_4$	N_2-Cd	30	6	0.36	7×10^{-5}
5-49-B	$GaCl_2$	N_2-Cd	--	--	< 0.1	$< 1 \times 10^{-6}$
5-49-A	$GaCl_2$	N_2	--	--	0.3	8×10^{-6}
7-19-A	$CdSO_4$	N_2-Cd	30	6	0.31	8×10^{-5}
7-19-B	$CdSO_4$	N_2-Cd	30	4	0.36	5×10^{-4}
7-19-C	$CdSO_4$	N_2-Cd	30	5	0.31	5×10^{-3}

* $SnO_{2(sb)}$ transparent conductive layer; indium-doped CdTe layer.

indicating that the sheet conductivity of the CdTe layers is high. [Most of these devices are made without a transparent conductor, as suggested by Nakayama.[9]]

We have prepared two sets of cells in which the major variables were the flux level in the CdTe and the heat treatment times. The results are shown in Table 22. None of the devices that were produced on substrates with an ITO layer showed a diode characteristic. We have produced diodes on transparent conductors (Sample 5-46-C in Table 21). However, we recently increased the CuCl and HCL content of the dip solution and increased the temperature from 70°C to 90°C, with the result that the short circuit current increased (see Tables 21 and 22). Now all of the ITO-based devices are shorted as a result of the increased Cu_2Te and the etching of pinholes by the HCl.

Table 22

INFLUENCE OF HIGH FLUX LEVEL IN CdTe

Sample	CdS Heat-treatment at 600°C (hours)*	CdTe Flux Level (percent by weight)	Heat-treatment at 720°C (hours)	V-I Characteristic	V_{oc} (V)	I_{sc} (mA)
7-31-A†	1	5	1/2	Diode	0.36	0.24
7-31-B†	1	10	1/2	Diode	0.41	0.74
7-35-A	1/2	5	1	Diode	0.32	0.18
7-35-B	1/2	10	1	Diode	0.22	0.31
7-35-A1‡	1/2	5	1	Ohmic	–	–
7-35-B1‡	1/2	10	1	Ohmic	–	–
7-39-A‡§	1/2	5	1	Ohmic	–	–
7-39-B‡§	1/2	10	1	Ohmic	–	–

*33 percent by weight $CdCl_2 \cdot 21/2\ H_2O$, 6 percent by weight $CdSo_4$, 10 ml propylene glycol.

†The V_{oc} and I_{sc} dated listed here are measured 3 weeks after preparation of cells and thus different from the original data.

‡ITO transparent conductor ~500 Ω/□ sheet resistance.

§CdS film, double thickness (40 nm).

VI THERMODYNAMIC CALCULATIONS

A. Introduction

During the past year, thermodynamic calculations were made on systems simulating the spray pyrolysis and subsequent heat treatment of $CuInS_2$, $CuInSe_2$ and CdS in order to analyze the effects of reactants and temperature on the resulting film compositions. Calculations were also made on conditions for doping CdS and CdTe with chlorine. Because of the large number of possible reaction products in the systems investigated, a "free-energy minimization" computer program ("SOLGASMIX-PV" devised by T.M. Besmann at Oak Ridge National Laboratories, report 1977: ORNL/TM-5775) was used in most of the calculations. The input data were the possible chemical species of the system under consideration, their enthalpies and entropies of formation, temperature, pressure, and quantities of elements in the reactants. The program calculated the equilibrium composition (pressures of gases and amounts of solids) of the system, at which its free energy was a minimum.

B. Spray Pyrolysis Production of $CuInS_2$

1. Approach

The SOLGASMIX-PV computer program was applied to the Cu-In-S problem. The input enthalpies and entropies of formation of the possible species are shown in Table 23.

We considered seven elements: Cu, In, S, O, Cl, H, distributed among one gas mixture (containing as many as eight gaseous species) and sixteen solid compounds. We had no information on $CuInS_2$, and considered $Cu_2S + In_2S_3$ as separate phases. We assumed a temperature of 500^oK and a pressure of 1 atmosphere.

Table 23

INPUT DATA FOR SOLGAS PROGRAM

Species	Heat of Formation, ΔH (joules/mole)	Entropy of Formation, $-\Delta S$ (joules/mole/deg)
H_2	0.	0.
O_2	0.	0.
Cl_2	0.	0.
S_2	0.12879×10^6	-0.16450×10^3
N_2	0.	0.
H_2O	-0.24189×10^6	0.44500×10^2
HCl	-0.92300×10^5	-0.10000×10^2
H_2S	-0.20500×10^5	-0.43500×10^2
Cu_2O	-0.16740×10^6	0.75600×10^2
CuO	-0.15530×10^6	0.92900×10^2
CuCl	-0.13730×10^6	0.58400×10^2
$CuCl_2$	-0.21760×10^6	0.14810×10^3
Cu_2S	-0.79500×10^5	-0.23000×10^2
CuS	-0.52300×10^5	-0.16000×10^1
In_2O_3	-0.92610×10^6	0.31530×10^3
InCl	-0.18620×10^6	0.74300×10^2
$InCl_2$	-0.36280×10^6	0.15860×10^3
$InCl_3$	-0.53730×10^6	0.25130×10^3
InS	-0.13390×10^6	0.20550×10^2
In_5S_6	-0.77400×10^6	0.10550×10^3
In_2S_3	-0.35570×10^6	0.47500×10^2
Cu	0.	0.
In	0.	0.
S	0.	0.

Table 24 lists the output for the case of one liter of solution:

- 55.5 moles H_2O
- 0.006 moles CuCl
- 0.006 mols $InCl_3$
- 0.036 moles H_2S
- 0.05 moles HCl.

From these we calculated the amounts of the various elements required and input these amounts in the second column. The computer calculations minimize the free energy by distributing the elements among the various compounds and lists how many moles of each compound are in the equilibrium mixture in the third column. The fourth column gives the pressures of gases. Table 24 shows that, at equilibrium all the water will vaporize and there will be HCl and H_2S in the gas. The solid expected is Cu_2S, with a trace of CuS plus In_2S_3 and some In_2O_3, all of which is in agreement with experiments.

Table 25 shows the result for a reduced amount of H_2O (by evaporation) but not the other materials. The result is that CuCl and $InCl_3$ form, which is an undesirable outcome. Table 26 shows that reducing the amount of HCl results in In_2O_3 formation. Table 27 shows the effect of increasing the amount of H_2S: the solids become converted to Cu_2S and In_2S_3 (i.e., $CuInS_2$).

These preliminary results indicate that excess sulfur over the stoichiometric quantity and dilution also reduces the oxygen and chlorine content of the deposit, but increased HCl reduces oxygen.

2. Calculation of the Conditions Under Which $CuInS_2$ Becomes Unstable

Thermodynamic calculations were made of the conditions under which, for various reasons, the sulfides become unstable. These calculations can provide some idea of how to change conditions to avoid regions of instability if they are encountered. Unfortunately, the thermodynamic

Table 24

OUTPUT OF FREE-ENERGY MINIMIZATION PROGRAM--
REFERENCE CONDITIONS
(500°K, 1 atmosphere)

Element/ Compound	Amount (mole)		Gas Pressure (atm)
	Entered	Calculated Equilibrium	
Gas Phase			
H_2	0.55561×10^{2}	0.38631×10^{-4}	0.69483×10^{-6}
O_2	0.27750×10^{2}	0.14779×10^{-31}	0.26582×10^{-33}
Cl_2	0.37002×10^{-1}	0.66424×10^{-18}	0.11947×10^{-19}
S_2	0.	0.52119×10^{-6}	0.93743×10^{-8}
N_2	0.70000×10^{-5}	0.70000×10^{-5}	0.12590×10^{-6}
H_2O	0.	0.55498×10^{2}	0.99820
HCl	0.	0.74005×10^{-1}	0.13311×10^{-2}
H_2S	0.	0.25872×10^{-1}	0.46534×10^{-3}
Solid Phase			
Cu_2O	0.	0.	---
CuO	0.	0.	---
CuCl	0.	0.	---
$CuCl_2$	0.	0.	---
Cu_2S	0.	0.29599×10^{-2}	---
CuS	0.	0.81177×10^{-4}	---
In_2O_3	0.	0.63804×10^{-3}	---
InCl	0.	0.	---
$InCl_2$	0.	0.	---
$InCl_3$	0.	0.	---
InS	0.	0.	---
In_5S_6	0.	0.	---
In_2S_3	0.	0.23630×10^{-2}	---
Cu	0.60010×10^{-2}	0.	---
In	0.60020×10^{-2}	0.	---
S	0.36003×10^{-1}	0.	---

Table 25

OUTPUT OF FREE-ENERGY MINIMIZATION PROGRAM--
REDUCED H_2O CONTENT
(500°K, 1 atmosphere)

Element/ Compound	Amount (mole)		Gas Pressure (atm)
	Entered	Calculated Equilibrium	
Gas Phase			
H_2	0.12500	0.21253×10^{-13}	0.14168×10^{-12}
O_2	0.50002×10^{-1}	0.42777×10^{-21}	0.28516×10^{-20}
Cl_2	0.37002×10^{-1}	0.55108×10^{-9}	0.36736×10^{-8}
S_2	0.	0.21077×10^{-5}	0.14050×10^{-4}
N_2	0.70000×10^{-5}	0.70000×10^{-5}	0.46663×10^{-4}
H_2O	0.	0.10000	0.66634
HCl	0.	0.49998×10^{-1}	0.33330
H_2S	0.	0.55106×10^{-9}	0.36734×10^{-8}
Solid Phase			
Cu_2O	0.	0.	---
CuO	0.	0.	---
CuCl	0.	0.60010×10^{-2}	---
$CuCl_2$	0.	0.	---
Cu_2S	0.	0.	---
CuS	0.	0.	---
In_2O_3	0.	0.	---
InCl	0.	0.	---
$InCl_2$	0.	0.	---
$InCl_3$	0.	0.60020×10^{-2}	---
InS	0.	0.	---
In_5S_6	0.	0.	---
In_2S_3	0.	0.	---
Cu	0.60010×10^{-2}	0.	---
In	0.60020×10^{-2}	0.	---
S	0.36003×10^{-1}	0.35999×10^{-1}	---

Table 26

OUTPUT OF FREE-ENERGY MINIMIZATION PROGRAM--
DECREASED HCl CONTENT
(500°K, 1 atmosphere)

Element/ Compound	Amount (mole)		Gas Pressure (atm)
	Entered	Calculated Equilibrium	
Gas Phase			
H_2	0.10000	0.23208×10^{-15}	0.23143×10^{-14}
O_2	0.50002×10^{-1}	0.23581×10^{-17}	0.23783×10^{-16}
Cl_2	0.12002×10^{-1}	0.60177×10^{-11}	0.60006×10^{-10}
S_2	0.	0.14090×10^{-5}	0.14050×10^{-4}
N_2	0.70000×10^{-5}	0.70000×10^{-5}	0.69801×10^{-4}
H_2O	0.	0.99730×10^{-1}	0.99447
HCl	0.	0.54597×10^{-3}	0.54442×10^{-2}
H_2S	0.	0.60175×10^{-11}	0.60004×10^{-10}
Solid Phase			
Cu_2O	0.	0.	---
CuO	0.	0.	---
CuCl	0.	0.60010×10^{-2}	---
$CuCl_2$	0.	0.	---
Cu_2S	0.	0.	---
CuS	0.	0.	---
In_2O_3	0.	0.91329×10^{-4}	---
InCl	0.	0.	---
$InCl_2$	0.	0.	---
$InCl_3$	0.	0.58193×10^{-2}	---
InS	0.	0.	---
In_5S_6	0.	0.	---
In_2S_3	0.	0.	---
Cu	0.60010×10^{-2}	0.	---
In	0.60020×10^{-2}	0.	---
S	0.36003×10^{-1}	0.36000×10^{-1}	---

Table 27

OUTPUT OF FREE-ENERGY MINIMIZATION PROGRAM--
INCREASED H_2S (THIOUREA)
(500°K, 1 atmosphere)

Element/ Compound	Amount (mole)		Gas Pressure (atm)
	Entered	Calculated Equilibrium	
Gas Phase			
H_2	0.17053	0.29925×10^{-2}	0.16616×10^{-1}
O_2	0.50020×10^{-1}	0.25024×10^{-43}	0.14394×10^{-42}
Cl_2	0.95025×10^{-2}	0.56551×10^{-21}	0.31399×10^{-20}
S_2	0.	0.14138×10^{-11}	0.78499×10^{-11}
Ar	0.70000×10^{-4}	0.70000×10^{-4}	0.38867×10^{-3}
H_2O	0.	0.10004	0.55546
HCl	0.	0.19005×10^{-1}	0.10552
H_2S	0.	0.57995×10^{-1}	0.33201
Solid Phase			
Cu_2O	0.	0.	---
CuO	0.	0.	---
CuCl	0.	0.	---
$CuCl_2$	0.	0.30050×10^{-2}	---
Cu_2S	0.	0.	---
CuS	0.	0.	---
In_2O_3	0.	0.	---
InCl	0.	0.	---
$InCl_2$	0.	0.	---
$InCl_3$	0.	0.	---
InS	0.	0.	---
In_5S_6	0.	0.	---
In_2S_3	0.	0.30100×10^{-2}	---
Cu	0.60100×10^{-2}	0.	---
In	0.60200×10^{-2}	0.	---
S	0.70030×10^{-2}	0.	---

data needed for exact calculations are not available, and we were only able to calculate general trends. Because there are no data for the compound $CuInS_2$, we have considered the behaviors of Cu_2S and In_2S_3 separately and assumed that they behave similarly in the compound $CuInS_2$. Another facet of the problem is the potential formation of solid solutions in which oxygen or chlorine replace sulfur in the compound. The absence of information about such solid solutions prevents a good treatment of those effects.

The results of the calculations are as follows:

Thermal Decomposition--If $CuInS_2$ is heated in vacuum, or in an inert gas such as nitrogen (which is thermodynamically equivalent to vacuum), sulfur can evaporate (as gaseous S_2) and leave the solid deficient in sulfur. We have no thermodynamic data for sulfur-deficient $CuInS_2$; accordingly, we have calculated the sulfur pressures generated in the formation of In_5S_6 from In_2S_3 and copper from Cu_2S. (These are the next lower compounds that would form and the calculated sulfur pressures are therefore an indication of the values that might be expected for thermal decomposition.)

For the equilibrium

$$10/3In_2\ S_3(s) = 4/3In_5\ S_6(s) + S_2(g) \quad ,$$

we calculate the following expression for the pressure of sulfur:

$$\log P(S_2,atm) = -14,800/T + 9.51 \quad .$$

For the equilibrium

$$2\ Cu_2S(s) = 4\ Cu(s) + S_2(g) \quad ,$$

we find

$$\log P(S_2,atm) = 6.19 - 15000/T \quad .$$

Those equations are shown in Figure 18, from which it is apparent that the sulfur pressure for In_2S_3 decomposition is greater than that for Cu_2S decomposition.

These results indicate that if a mixture of Cu_2S and In_2S_3 were heated under inert conditions (vacuum or N_2 atmosphere), the In_2S_3 would lose sulfur more readily than Cu_2S.

Loss of sulfur from the compound $CuInS_2$ to form a sulfur-deficient structure ($CuInS_{x-2}$) would be expected to occur more readily than decomposition of In_2S_3. Thus it is anticipated that sulfur pressures for the compound would be larger than the upper curve of Figure 18. We cannot give a good estimate of how much larger at present because of the lack of good information.

Pressure of H_2S Required to Prevent Thermal Decomposition--The thermal decomposition of sulfides heated in vacuum can be suppressed by imposing a pressure of H_2S. The relevant equations are

$$5/3\ In_2S_3(s) + H_2(g) = 2/3\ In_5S_6(s) + H_2S(g) \quad ,$$

for which

$$\log\left[\frac{P(H_2S)}{P(H_2)}\right] = 2.73 - 2900/T \quad ;$$

and

$$Cu_2S(s) + H_2(g) = 2\ Cu(s) + H_2S(g) \quad ,$$

for which

$$\log\left[\frac{P(H_2S)}{P(H_2)}\right] = 1.07 - 3100/T \quad .$$

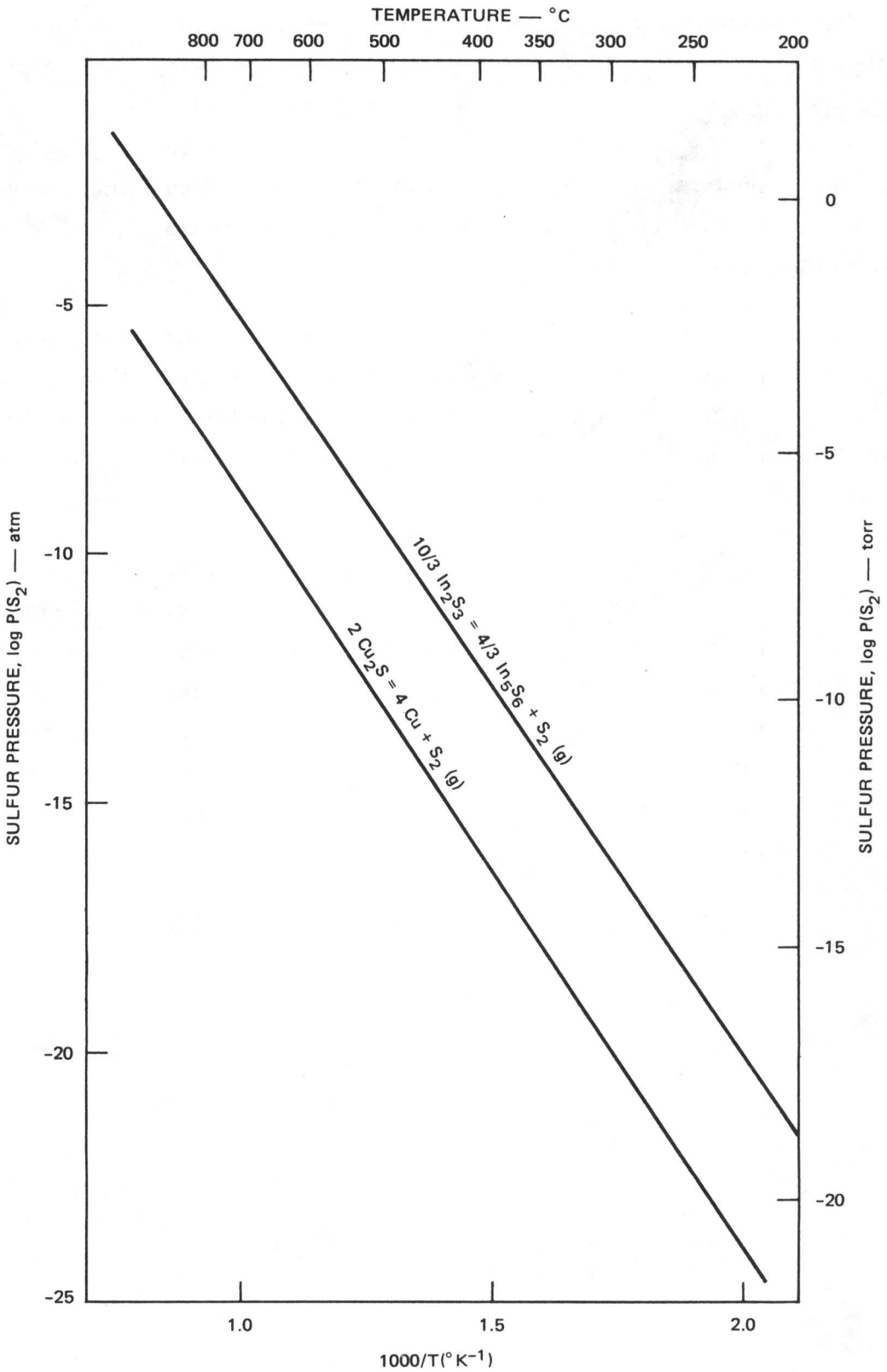

FIGURE 18 PARTIAL PRESSURE OF SULFUR (S_2) IN EQUILIBRIUM WITH In_2S_3/In_5S_6 AND Cu_2S/Cu AS A FUNCTION OF TEMPERATURE

The reactions involve both H_2S and H_2; their ratio determines whether the reaction will go to the right or to the left. The above equations for pressure ratios are plotted in Figure 19. Values of the ratios of H_2S/H_2above a line in Figure 19 would cause the particular reaction to go to the left as written. The data in Figure 19 show that a higher H_2S/H_2 ratio is required to suppress the decomposition of In_2S_3 than for Cu_2S.

Here again, the existence of a sulfur-deficient compound would influence the interpretation. Loss of sulfur by $CuInS_2$ to form $CuInS_{2-x}$ would probably occur at higher H_2S/H_2 ratios that those indicated by the upper line in Figure 19; the exact ratios cannot be evaluated at present for want of data.

Substitution of Sulfur by Oxygen--Another possibility is that oxygen can substitute for sulfur in $CuInS_2$ and alter its electronic properties. Figure 20 shows calculations of the H_2S/H_2O ratio in equilibrium with In_2S_3/In_2O_3 and Cu_2S/Cu_2O. In effect, it gives the ratios of H_2S/H_2O in the gas phase needed to prevent conversion of the sulfides to the oxides. For In_2S_3, the ratio is larger than for Cu_2S, which means it is easier to convert the indium sulfide to oxide than copper. The equations are:

$$1/3\ In_2S_3(s) + H_2O(g) = 1/3\ In_2O_3(s) + H_2S(g) \quad ,$$

$$\text{Log}\left[\frac{P(H_2S)}{P(H_2O)}\right] = -1600/T \quad ,$$

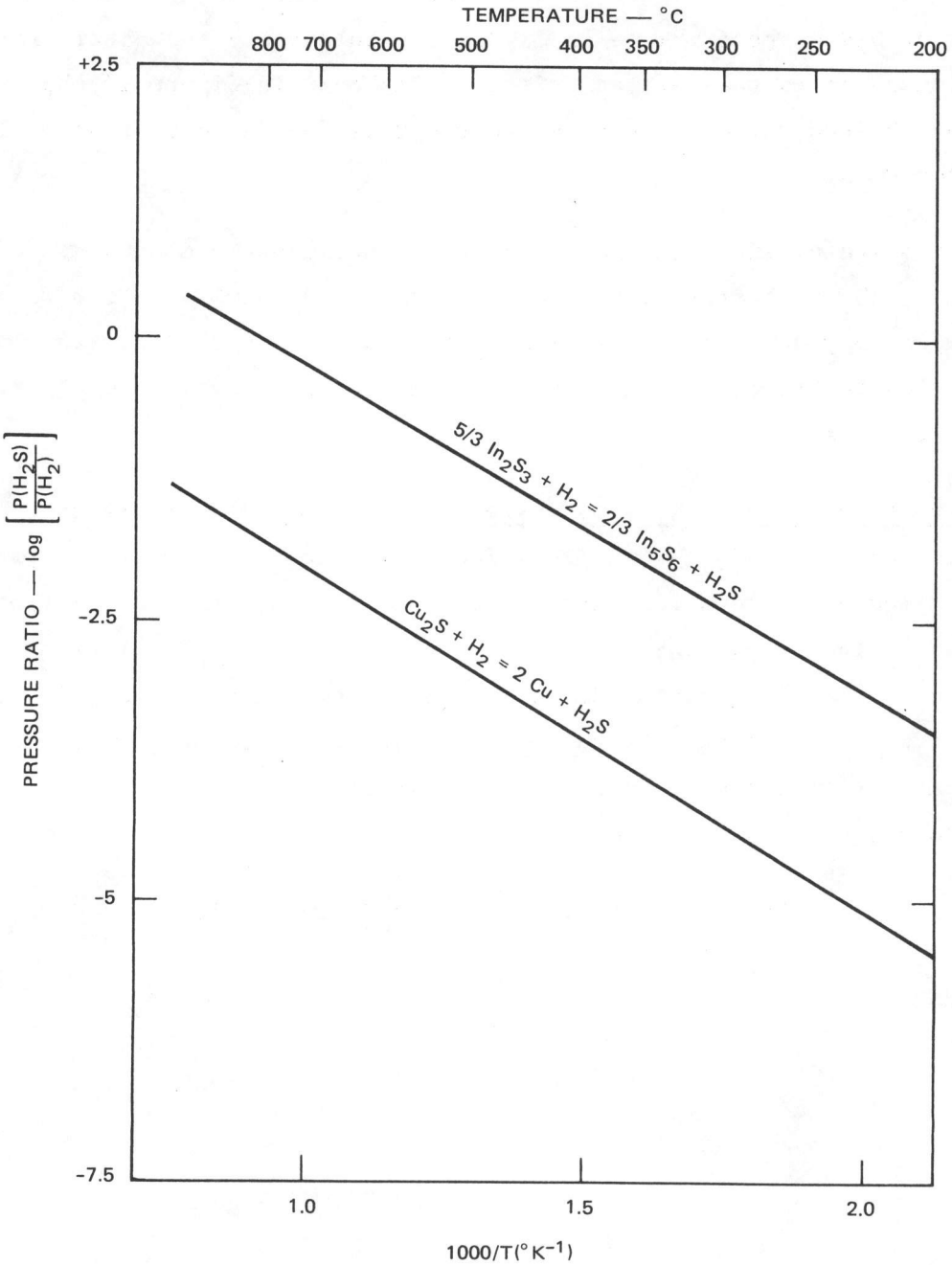

FIGURE 19 RATIOS OF PRESSURES OF H_2S/H_2 IN EQUILIBRIUM WITH In_2S_3/In_5S_6 AND Cu_2S/Cu

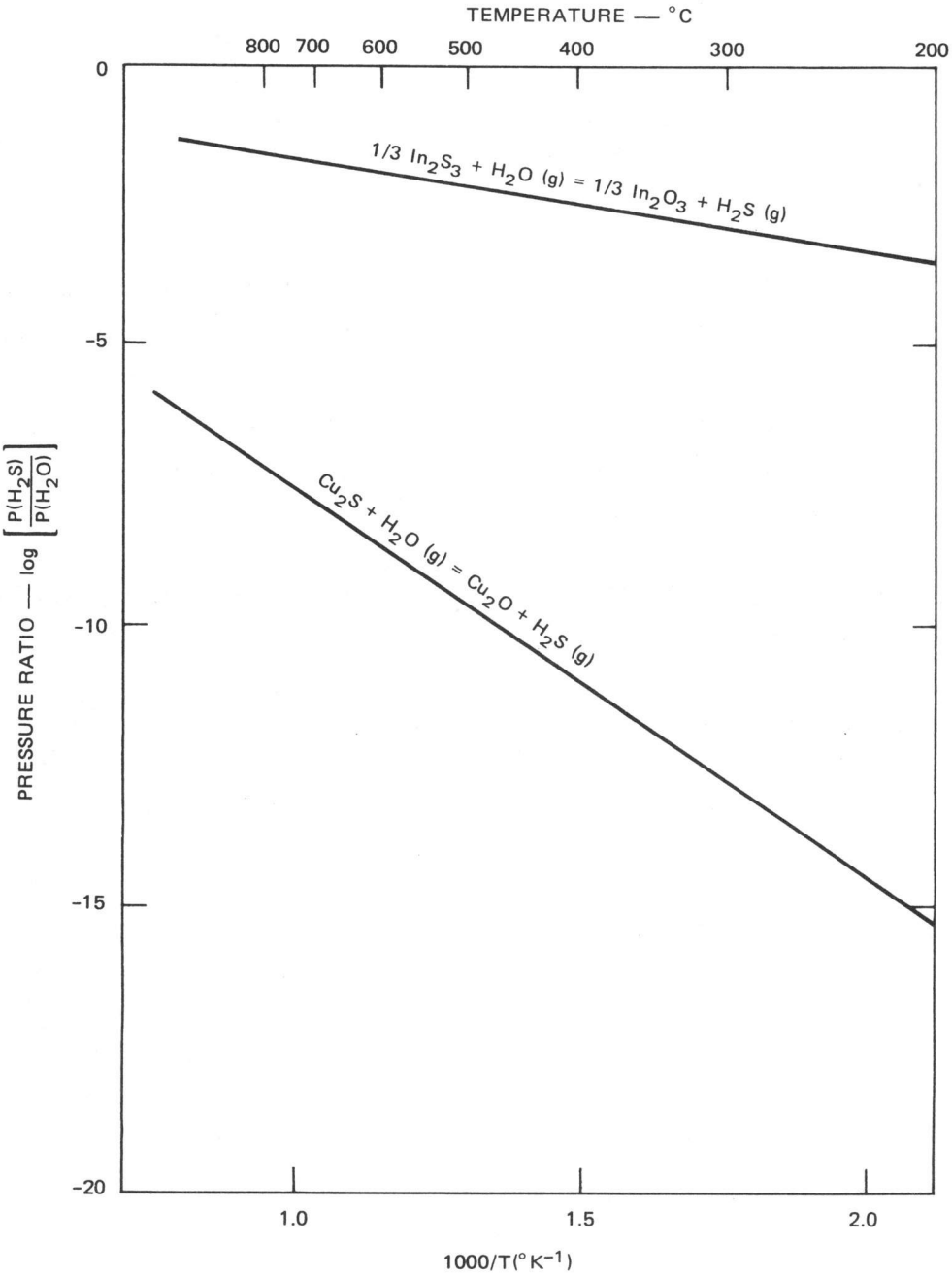

FIGURE 20 RATIOS OF PRESSURES OF H_2S/H_2O IN EQUILIBRIUM WITH INDIUM AND COPPER SULFIDES AND OXIDES

and

$$Cu_2S(s) + H_2O(g = Cu_2O(s) + H_2S(g) \quad ;$$

$$\text{Log}\left[\frac{P(H_2S)}{P(H_2O)}\right] = -0.56 - 7000/T \quad .$$

This calculation is also only a lower limit because we are considering the complete conversion of In_2S_3 and In_2O_3. In the real system, solid solutions of the type $CuInS_{2-y}O_y$ could probably form more easily than the complete conversion. Thus, the incorporation of oxygen impurities in solid solution might occur at H_2S/H_2 ratios that were orders of magnitude larger than the Figure 20 values.

Substitution of Sulfur by Chlorine--There is also the possibility that chlorine can substitute for sulfur in the compound. The equilibrium calculations for the conversion from sulfide to chloride are shown in Figure 21. The relevant equations are:

$$1/3\ In_2S_3(s) + 2\ HCl(g) = 2/3\ InCl_3(s) + H_2S(g) \quad ,$$

$$\text{Log}\left[\frac{P(H_2S)}{P^2(HCl)}\right] = 1970/T - 3.34 \quad ,$$

$$Cu_2S(s) + 2\ HCl(g) = 2\ CuC(s) + H_2S(g) \quad ,$$

$$\text{Log}\left[\frac{P(H_2S)}{P^2(HCl)}\right] = 800/T - 3.03 \quad .$$

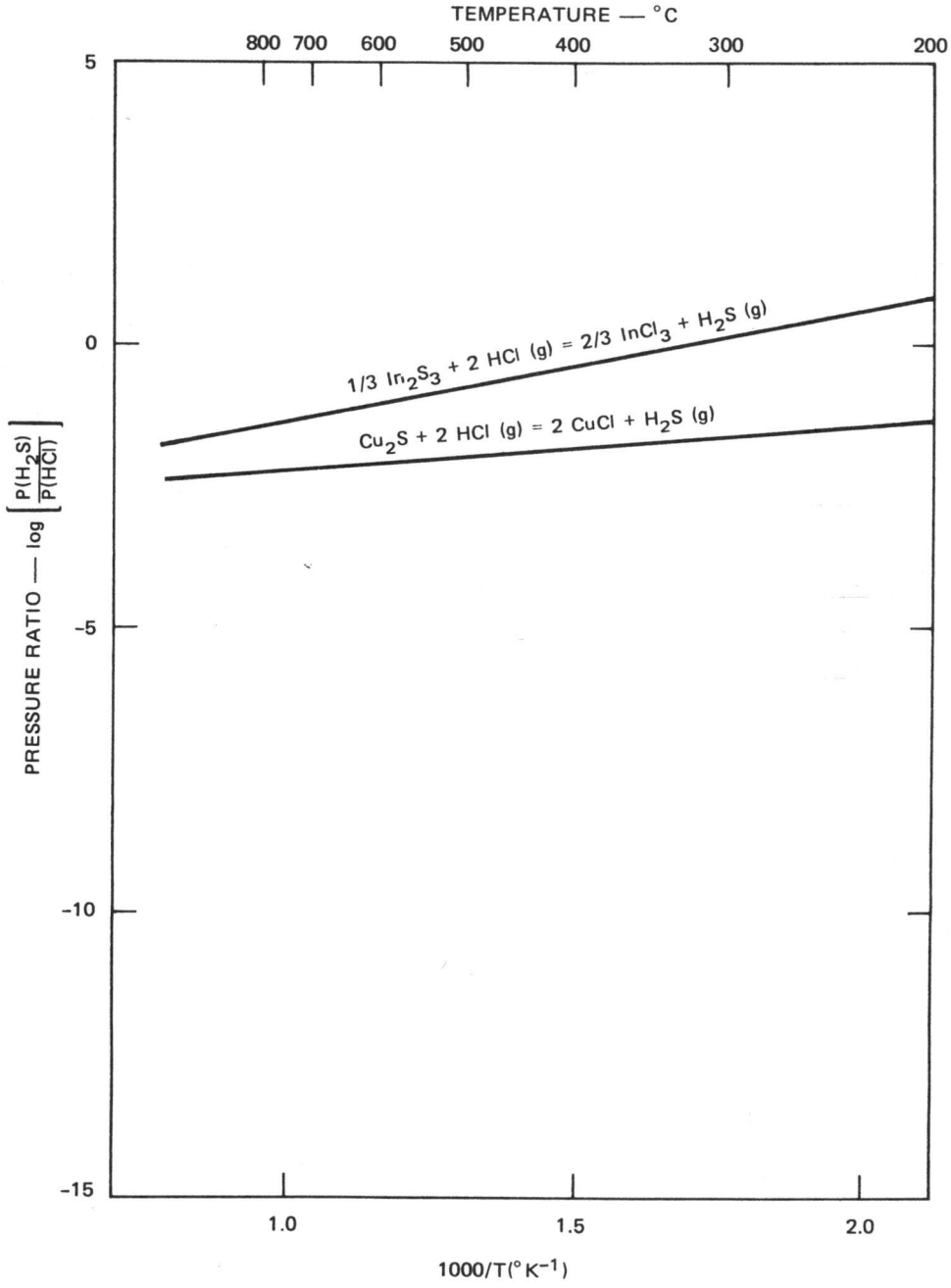

FIGURE 21 RATIOS OF PRESSURES OF H_2S AND HCl IN EQUILIBRIUM WITH INDIUM AND COPPER SULFIDES AND CHLORIDES

The caveat about solid solutions of the type $CuInS_{2-z}Cl_{2z}$ applies and for the real system, the values in Figure 21 are again essentially a lower limit.

C. Calculations of Doping Conditions for CdS and CdTe

We can approximate the conditions for doping materials from thermodynamic considerations; however, the data needed for accurate evaluations are generally not available. For doping CdS with chlorine, we make the following calculations. For the equilibrium

$$CdS(s) + 2\ HCl(g) = CdCl_2(s) + H_2S(g) \quad ,$$

we calculate for the equilibrium constant, K,

$$\text{Log } K = 4000/T - 6.32 \quad .$$

The equilibrium constant expression is

$$K = \frac{a(CdCl_2) \cdot P(H_2S)}{a(CdS) \cdot P^2(HCl)} \quad .$$

For a CdS crystal, a(CdS) is unity. We shall assume that the activity of $CdCl_2$ is given by the following expression:

$$a_{CdCl_2} = X_{Cd} \cdot Y_{Cl}^2 \quad ,$$

where X_{Cd} is the atom fraction of cadmium in the metal sublattice (X_{Cd} - 1 for chlorine doping) and Y_{Cl} is the atom fraction of Cl on the anion sublattice. Thus, the equilibrium constant becomes

$$K = \frac{Y_{Cl}^2 P(H_2S)}{P^2(HCl)} \quad .$$

For 0.1 percent chlorine doping, $Y = 10^{-3}$ and

$$K^{-1} = 10^{-6} \frac{P(H_2S)}{P^2(HCl)} ,$$

so that

$$\text{Log} \frac{P(H_2S)}{P^2(HCl)} = 4000/T - 0.32$$

for chlorine doping at the 0.1-percent level according to this treatment. For larger ratios of $P(H_2S)/P^2(HCl)$, the amount of chlorine would be smaller and vice versa.

For doping CdTe with indium using $InCl_3$ vapor, the following equilibrium can be considered:

$$CdTe(s) + InCl_3(g) + 3/2\ H_2(g) = Cd(s) + 3\ HCl(g) + InTe(s) ,$$

for which $\log K = 10.36 - 12700/T$.

For this equilibrium to hold, the pressure of $InCl_3$ must not exceed its vapor pressure. Other equilibria must be considered for those cases. Those vapor pressures are given by

$$\log P(InCl_3, atm) = 10.74 - 8270/T .$$

The equilibrium constant for the above equilibrium is given by

$$K = \frac{a(InTe)a(Cd)\ P^3(HCl)}{a(CdTe)\ P(InCl_3)P^{3/2}(H_2)} .$$

We shall assume that:

- a(CdTe) = 1 (i.e., host crystal).
- a(Cd) = 1 (i.e., cadmium leaves the crystal to form a separate phase).
- $a(InTe) = X_{In}\, Y_{Te} = X_{In}$.

Then, for 0.1 percent In in CdTe, $X_{In} = 10^{-3}$ and

$$K_1 = 10^{-3} \frac{P^3(HCl)}{P(InCl_3)P^{3/2}(H_2)} ,$$

which becomes

$$\log \frac{P^3(HCl)}{P(InCl_3)P^{3/2}(H_2)} = 13.36 - 12700/T \quad .$$

This relation gives the conditions under which we anticipate 0.1-percent indium doping In CdTe, based on the assumptions made.

In both cases of doping treated, the expressions derived depend on activity coefficients that we have assumed to be unity. Therefore, the expressions are inaccurate numerically but give the form of the relationships of applied gas pressures.

D. Spray Pyrolysis Production and Heat Treatment of $CuInSe_2$

The SOLGASMIX-PV "free-energy minimization" computer program was applied to the Cu-In-Se problem. In this program, the heats of formation and entropies of all possible compounds among the elements of interest, as listed in Table 28, are entered. Fixed amounts of the elements are then input, and the program prints out the calculated pressures of gases and the amounts of solids in the equilibrium mixture.

We considered seven elements--copper, indium, selenium, oxygen, chlorine, hydrogen, and nitrogen--distributed among one gas mixture (containing as many as eight gaseous species) and eighteen solid

Table 28

INPUT DATA FOR SOLGASMIX-PV PROGRAM

Species	Heat of Formation (J/mole)	Entropy of Formation, Δ J/mole·deg
H_2	0.	0.
O_2	0.	0.
Cl_2	0	0.
Se_2	0.13933×10^6	-0.1590×10^3
H_2O	-0.24189×10^6	0.4450×10^2
HCl	-0.92300×10^5	-0.1000×10^2
H_2Se	0.29290×10^5	-0.4600×10^2
N_2	0.	0.
Cu_2O	-0.16740×10^6	0.7560×10^2
CuO	-0.15530×10^6	0.9290×10^2
CuCl	-0.13730×10^6	0.5840×10^2
$CuCl_2$	-0.21760×10^6	0.1481×10^3
Cu_2Se	-0.65270×10^5	-0.2120×10^2
CuSe	-0.41840×10^5	-0.2800×10^1
$CuSeO_4$	-0.49580×10^6	$0.3637 \times 10^{3*}$
In_2O_3	-0.92610×10^6	0.3153×10^3
InCl	-0.18620×10^6	0.7430×10^2
$InCl_2$	-0.36280×10^6	0.1586×10^3
$InCl_3$	-0.53730×10^6	0.2513×10^3
InSe	-0.11800×10^6	0.1850×10^2
In_5Se_6	$-0.68032 \times 10^{6*}$	$0.9720 \times 10^{2*}$
In_2Se_3	-0.32635×10^6	0.4120×10^2
$In_2(SeO_4)_3$	$-0.18240 \times 10^{7*}$	$0.1133 \times 10^{4*}$
Cu	0.	0.
In	0.	0.
Se	0.	0.

*Estimated

compounds. We have no information on $CuInSe_2$ yet, and for the present are considering Cu_2Se and In_2Se_3 as separate phases. We assume a temperature of 500°K and a pressure of 1 atmosphere.

Table 29 lists the output for the case of 1 liter of solution from which most of the water (but none of the other materials) has been lost by evaporation. Excess H_2Se above the amount needed to form Cu_2Se and In_2Se_3 is present. The input data correspond to:

- 0.100 H_2O
- 0.006 CuCl
- 0.006 $InCl_3$
- 0.070 H_2Se
- 0.074 HCl
- 0.050 N_2

The program output shows that In_2Se_3 is a stable product under these conditions, but that CuSe (rather than Cu_2Se) is thermodynamically preferred. Also, solid selenium is calculated to result from the establishment of the $H_2Se = H_2 + Se$ equilibrium.

Table 30 gives the equilibrium composition of an input mixture identical to that of Table 28, except that the N_2 gas contains 10 molecular percent O_2 as an impurity. The output indicates that this extra oxygen is converted to water vapor at the expense of H_2Se and H_2. A greater amount of solid selenium is present, because more H_2Se has dissociated to establish the $H_2Se = H_2 + Se$ equilibrium.

Table 31 shows the effect of eliminating excess H_2Se in the input mixture. The reduced selenium activity leads to a mixture of Cu_2Se and CuSe, but also to $InCl_3$, as well as In_2Se_3. Table 32 shows the effect of excess O_2 in the input mixture when no excess H_2Se is present. Instead of forming selenides, both $CuSeO_4$ and $In_2(SeO_4)_3$ are formed, along with In_2Cl_3. Excess H_2Se suppresses the formation of selenates by removing the excess O_2 to form water vapor.

Table 29

OUTPUT OF FREE-ENERGY MINIMIZATION PROGRAM—EXCESS H_2Se, NO EXCESS O_2
500°K, 1 atmosphere

Element/Compound	Amount (mole)		Gas Pressure (atm)
	Entered	Calculated Equilibrium	
Gas Phase			
H_2	0.1950	0.4753×10^{-1}	0.1686
O_2	0.5000×10^{-1}	0.1604×10^{-45}	0.5689×10^{-45}
Cl_2	0.3700×10^{-1}	0.5394×10^{-21}	0.1913×10^{-20}
Se_2	0.	0.1585×10^{-6}	0.5619×10^{-6}
H_2O	0.	0.1000	0.3546
HCl	0.	0.7400×10^{-1}	0.2624
H_2Se	0.	0.1047×10^{-1}	0.3712×10^{-1}
N_2	0.5000×10^{-1}	0.5000×10^{-1}	0.1773
Solid Phase			
Cu_2O	0.	0.	
CuO	0.	0.	
CuCl	0.	0.	
$CuCl_2$	0.	0.	
Cu_2Se	0.	0.	
CuSe	0.	0.6001×10^{-2}	
$CuSeO_4$	0.	0.	
In_2O_3	0.	0.	
InCl	0.	0.	
$InCl_2$	0.	0.	
In_3Cl	0.	0.	
InSe	0.	0.	
In_5Se_6	0.	0.	
In_2Se_3	0.	0.3001×10^{-2}	
$In_2(SeO_4)_3$	0.	0.	
Cu	0.6001×10^{-2}	0.	
In	0.6002×10^{-2}	0.	
Se	0.7003×10^{-1}	0.4456×10^{-1}	

Table 30

OUTPUT OF FREE-ENERGY MINIMIZATION PROGRAM—EXCESS H_2Se, EXCESS O_2
500°K, 1 atmosphere

Element/Compound	Amount (mole)		Gas Pressure (atm)
	Entered	Calculated Equilibrium	
Gas Phase			
H_2	0.1950	0.3934×10^{-1}	0.1420
O_2	0.5500×10^{-1}	0.2784×10^{-45}	0.1005×10^{-44}
Cl_2	0.3700×10^{-1}	0.6517×10^{-21}	0.2353×10^{-20}
Se_2	0.	0.1556×10^{-6}	0.5619×10^{-6}
H_2O	0.	0.1100	0.3971
HCl	0.	0.7400×10^{-1}	0.2672
H_2Se	0.	0.8664×10^{-2}	0.3128×10^{-1}
N_2	0.4500×10^{-1}	0.4500×10^{-1}	0.1625
Solid Phase			
Cu_2O	0.	0.	
CuO	0.	0.	
CuCl	0.	0.	
$CuCl_2$	0.	0.	
Cu_2Se	0.	0.	
CuSe	0.	0.6001×10^{-2}	
$CuSeO_4$	0.	0.	
In_2O_3	0.	0.	
InCl	0.	0.	
$InCl_2$	0.	0.	
$InCl_3$	0.	0.	
InSe	0.	0.	
In_5Se_6	0.	0.	
In_2Se_3	0.	0.3001×10^{-2}	
$In_2(SeO_4)_3$	0.	0.	
Cu	0.6001×10^{-2}	0.	
In	0.6002×10^{-2}		
Se	0.7003×10^{-1}	0.4636×10^{-1}	

Table 31

OUTPUT OF FREE-ENERGY MINIMIZATION PROGRAM—NO EXCESS H_2Se, NO EXCESS O_2
500°K, 1 atmosphere

Element/Compound	Amount (mole)		Gas Pressure (atm)
	Entered	Calculated Equilibrium	
Gas Phase			
H_2	0.1370	0.1437×10^{-2}	0.6457×10^{-2}
O_2	0.5000×10^{-1}	0.1385×10^{-42}	0.6225×10^{-42}
Cl_2	0.3700×10^{-1}	0.1646×10^{-19}	0.7396×10^{-19}
Se_2	0.	0.7590×10^{-9}	0.3411×10^{-8}
H_2O	0.	0.1000	0.4494
HCl	0.	0.7108×10^{-1}	0.3194
H_2Se	0.	0.2466×10^{-4}	0.1108×10^{-3}
N_2	0.5000×10^{-1}	0.5000×10^{-1}	0.2247
Solid Phase			
CuO_2	0.	0.	
CuO	0.	0.	
CuCl	0.	0.	
$CuCl_2$	0.	0.	
Cu_2Se	0.	0.1567×10^{-2}	
CuSe	0.	0.2867×10^{-2}	
$CuSeO_4$	0.	0.	
In_2O_3	0.	0.	
InCl	0.	0.	
$InCl_2$	0.	0.	
$InCl_3$	0.	0.9744×10^{-3}	
InSe	0.	0.	
In_5Se_6	0.	0.	
In_2Se_3	0.	0.2514×10^{-2}	
$In_2(SeO_4)_3$	0.	0.	
Cu	0.6001×10^{-2}	0.	
In	0.6002×10^{-2}	0.	
Se	0.1200×10^{-1}	0.	

Table 32

OUTPUT OF FREE ENERGY MINIMIZATION PROGRAM--NO EXCESS H_2Se, EXCESS O_2
500°K, 1 atmosphere

Element/Compound	Amount (mole)		Gas Pressure (atm)
	Entered	Calculated Equilibrium	
Gas Phase			
H_2	0.1370	0.3034×10^{-19}	0.1376×10^{-18}
O_2	0.7500×10^{-1}	0.3343×10^{-9}	0.1517×10^{-8}
Cl_2	0.3700×10^{-1}	0.6631×10^{-3}	0.3008×10^{-2}
Se_2	0.	0.1239×10^{-6}	0.5619×10^{-6}
H_2O	0.	0.1042	0.4728
HCl	0.	0.6556×10^{-1}	0.2974
H_2Se	0.	0.6683×10^{-20}	0.3152×10^{-19}
N_2	0.5000×10^{-1}	0.5000×10^{-1}	0.2268
Solid Phase			
CuO_2	0.	0.	
CuO	0.	0.	
CuCl	0.	0.	
$CuCl_2$	0.	0.	
Cu_2Se	0.	0.	
CuSe	0.	0.	
$CuSeO_4$	0.	0.6001×10^{-2}	
In_2O_3	0.	0.	
InCl	0.	0.	
$InCl_2$	0.	0.	
$InCl_3$	0.	0.1814×10^{-2}	
InSe	0.	0.	
In_5Se_6	0.	0.	
In_2Se_3	0.	0.	
$In_2(SeO_4)_3$	0.	0.1814×10^{-2}	
Cu	0.6001×10^{-2}	0.	
In	0.6002×10^{-2}	0.	
Se	0.1200×10^{-1}	0.5554×10^{-3}	

A final computer calculation was made with the conditions of Table 29, except that 10 molecular percent H_2 was present in the N_2. The result was that the dissociation of H_2Se into H_2 and solid selenium was slightly suppressed; however, CuSe was still obtained, rather than Cu_2Se.

Calculations were made for individual reactions to indicate regions of stability for the desired products (Cu_2Se and In_2Se_3) and conditions under which CuSe would be converted to Cu_2Se. These results are summarized as follows:

- Thermal decomposition of Cu_2Se and In_2Se_3 should not be a problem below 500°C.
- Free oxygen will react with Cu_2Se and In_2Se_3 to form $CuSeO_4$ and $In_2(SeO_4)_3$ in the absence of competing reactions that preferentially react with O_2. Any heat treatment or hydrogen baking of deposited layers should avoid the presence of O_2.
- Hydrogen baking of Cu_2Se and In_2Se_3 will not reduce the selenides to copper or In_5Se_6.
- The vapor pressure of Se_2 gas in equilibrium with solid selenium is 1.003 atm at 400°C and 0.077 atm at 500°C; therefore, vacuum annealing may be considered as a means of removing elemental selenium from deposited layers.
- The vapor pressure of Se_2 gas in equilibrium with both solids in the reaction $2\ CuSe = Cu_2Se + 1/2\ Se_2$ is 2×10^{-4} atm at 400°C and 1×10^{-2} atm at 500°C. Vacuum annealing should be considered to convert CuSe to Cu_2Se.
- The ratio $p(H_2Se)/p(H_2)$ for equilibrium in the reaction $2\ CuSe + H_2 = Cu_2Se + H_2Se$ is 0.32 at 400°C and 0.98 at 500°C. The ratio $p(H_2Se)/H_2)$ for equilibrium in the reaction $5/3\ In_2Se_3 + 2/3\ In_5Se_6 + H_2Se$ is 2.1×10^{-7} at 400°C and 3.3×10^{-6} at 500°C. Hydrogen baking should convert CuSe to Cu_2Se without reducing In_2Se_3 to In_2Se_6.

The caveats about thermodynamic calculations made for the solid sulfides mentioned earlier are also applicable to the solid selenide data here. The existence of selenium-deficient compounds could lead to greater losses of selenium than mentioned above. The data needed for more precise calculations do not exist, and the results presented should be considered indicative of general trends, rather than exact predictions.

Also, spray pyrolysis is a dynamic (rather than equilibrium) process; the exact compositions of reactants and products at the reaction surface may not be those predicted by thermodynamic considerations. For instance, copper may be deposited primarily in the cuprous state rather than the cupric state predicted by thermodynamic calculations. Predictions about vacuum annealing and hydrogen baking, which may be done under more controlled conditions, are more certain, not forgeting the possible effect of selenium-deficient compounds.

E. Spray Pyrolysis Production of CdS

The SOLGASMIX-PV free energy minimization computer program was used to analyze the thermodynamic equilibria applicable to the spray pyrolysis production of CdS. In this program, the heats and entropies of formation are entered for all possible compounds of interest, as listed in Table 33. Fixed amounts of the elements, corresponding to the elemental composition of the starting materials, are entered. The program prints out the calculated pressures of gases and amounts of solids in the equilibrium products.

We considered six elements--cadmium, sulfur, oxygen, chlorine, hydrogen, nitrogen--distributed among one gas mixture (containing as many as eight gaseous species) and six solid species. We assumed a temperature of 500°K and a total pressure of 1 atmosphere.

We calculated equilibria for three basic sets of conditions:

- Condition A--concentration of $CdCl_2$ was 0.010 molar.
- Condition B--Concentration of $CdCl_2$ was effectively increased by the evaporation of water.
- Condition C--Concentration of $CdCl_2$ was 0.005 molar.

Additionally, within these basic conditions, ratios of $CdCl_2$ to H_2S (representing thiourea) were changed as required to get CdS as an essentially pure solid product, and the effect of changing the propellant gas to 10 mol/percent H_2:90 mol/percent O_2 was investigated. The program inputs and calculated equilibria are given in Tables 34 and 35.

Table 33

INPUT DATA FOR SOLGASMIX-PV PROGRAM

Species	Heat of Formation (J/mol)	Entropy of Formation [J/(mol/deg)]
H_2, g	0	0
O_2, g	0	0
Cl_2, g	0	0
S_2, g	128700.	-164.5
N_2, g	0	0
H_2O, g	-241890.	44.5
HCl, g	-92300.	-10.0
H_2S, g	-20500.	-43.5
$CdCl_2$, s	-390800.	159.5
CdS, s	-149400.	14.6
$CdSO_4$, s	-928900.	370.7
CdO, s	-259400.	99.5
Cd, s	0	0
S, s	0	0

Table 34

SOLGASMIX-PV REACTANTS—CdS

Conditions	Reactants (mol)				
	H_2O	$CdCl_2$	H_2S	N_2	H_2
A 0.01 mol $CdCl_2$					
1 Reference	27.754	5.00×10^{-3}	5.00×10^{-3}	4.87×10^{-2}	--
2 1.3 $H_2S/CdCl_2$	27.754	5.00×10^{-3}	5.00×10^{-3}	4.87×10^{-2}	--
B H_2O Lowered (evaporation)					
1 2 $H_2S/CdCl_2$	1.00×10^{-1}	5.00×10^{-3}	1.00×10^{-2}	4.87×10^{-2}	--
2 5 $H_2S/CdCl_2$	1.00×10^{-1}	5.00×10^{-3}	2.50×10^{-2}	4.87×10^{-2}	--
3 10 $H_2S/CdCl_2$	1.00×10^{-1}	5.00×10^{-3}	5.00×10^{-2}	4.87×10^{-2}	--
C 0.005 mol $CdCl_2$					
1 Reference	27.754	2.50×10^{-3}	2.50×10^{-3}	4.87×10^{-2}	--
2 1.3 $H_2S/CdCl_2$	27.754	2.50×10^{-3}	3.25×10^{-3}	4.87×10^{-2}	--
3 10% H_2/90% N_2 Propellant	27.754	2.50×10^{-3}	2.50×10^{-3}	4.38×10^{-2}	4.87×10^{-3}
4 0.8$H_2S/CdCl_2$	27.754	2.50×10^{-3}	2.00×10^{-3}	4.87×10^{-2}	--
5 0.8 $H_2S/CdCl_2$, 10% H_2 Propellant	27.754	2.50×10^{-3}	2.00×10^{-3}	4.38×10^{-2}	4.87×10^{-3}
D 1.0 $CdCl_2$/0.9 H_2S	55.508	0.005	0.0045	0.817	–
E 1.0 $CdCl_2$/1.0 H_2S	55.508	0.005	0.005	0.817	–
F D + 90% N_2/10% H_2	55.508	0.005	0.0045	0.7355	0.0817

Table 35

SOLGASMIX-PV SOLID PRODUCTS—CdS

Conditions	Products			
	CdS	$CdCl_2$	$CdSO_4$	S
A 0.01 mol $CdCl_2$				
1 Reference	4.82×10^{-3}	1.81×10^{-4}	4.02×10^{-7}	–
2 1.3 $H_2S/CdCl_2$	5.00×10^{-3}	–	4.02×10^{-7}	–
B H_2 lowered (evaporation)				
1 2 $H_2S/CdCl_2$	2.38×10^{-3}	2.62×10^{-3}	–	2.94×10^{-7}
2 5 $H_2S/CdCl_2$	4.14×10^{-3}	8.64×10^{-4}	–	8.05×10^{-7}
3 10 H_2/CdCl2	5.00×10^{-3}	–	–	1.74×10^{-6}
C 0.005 mol $CdCl_2$				
1 Reference	2.45×10^{-3}	4.69×10^{-5}	4.03×10^{-7}	–
2 1.3 $H_2S/CdCl_2$	2.50×10^{-3}	–	–	–
3 10% H_2/90% N_2 Propellant	2.45×10^{-3}	4.69×10^{-5}	–	–
4 0.8 $H_2S/CdCl_2$	1.97×10^{-3}	4.69×10^{-5}	–	–
5 0.8 $H_2/CdCl_2$, 10% H_2 Propellant	1.97×10^{-3}	5.30×10^{-4}	–	–
D 1.0 $CdCl_2$/0.9 H_2S				
1 225°C = 498K	4.42×10^{-3}	5.82×10^{-4}	7.68×10^{-7}	–
2 325°C = 598K	4.49×10^{-3}	5.04×10^{-3}	5.13×10^{-6}	
E 1.0 $CdCl_2$/1.0 H_2S				
1 225°C = 498K	4.90×10^{-3}	1.01×10^{-4}	7.68×10^{7}	–
2 325°C = 598K	4.99×10^{-3}	4.62×10^{-6}	5.13×10^{-6}	–
F D + 90% N_2/10% H_2				
1 225°C = 498K	4.42×10^{-3}	5.82×10^{-4}	–	–
2 325°C = 598K	4.50×10^{-3}	$5.-4 \times 10^{-3}$	–	–

Conditions A and C, in our opinion, are more representative of conditions at the pyrolysis surface than is Condition B. During spray deposition, the gas phase near the surface should be dominated by the large volume of evaporated water. The results can be interpreted as follows:

- The more dilute solution (0.005 mol $CdCl_2$) with a slight excess of H_2S led to the quantitative production of CdS.
- The more concentrated solution (0.010 mol $CdCl_2$) with the same relative excess of CdS produced CdS with a trace amount of $CdSO_4$.
- The very concentrated solutions produced by water evaporation from spray solutions gave pure CdS (with traces of sulfur) only at very high H_2S:$CdCl_2$ ratios (10:1).
- Addition of H_2 to the propellant suppressed $CdSO_4$ where it was present in trace quantities, but had no effect on $CdCl_2$ production.

Table 36 gives a detailed output of the program for Condition C.

Subsequent to the above calculations, we calculated the products for the following conditions (1 liter of solution):

- Condition D--0.005 M $CdCl_2$, 0.0045 M H_2S (thiourea) at 225 and 325°C.
- Condition E--0.005 M $CdCl_2$, 0.005 M H_2S (thiourea) at 225 and 325°C.
- Condition F--D + 90% N_2 - 10% H_2 propellant at 225 and 325°C.

These calculations indicated that under Condition D there was little temperature dependence of the amount of $CdCl_2$ produced, while the amount of $CdSO_4$ produced was about six times greater at the higher temperature. Under Condition E, the amount of $CdCl_2$ produced was a factor of 22 lower at 325°C than at 225°C, while the amount of $CdSO_4$ was the same as for condition D. Condition F yielded the same results as condition D, except that no sulfate was produced.

Table 36

OUTPUT OF SOLGASMIX-PV FOR CONDITION C.2 OF TABLE 35

Element/ Compound	Amount (mol)		
	As Entered	Calculated Equilibrium	Under Pressure
Gas Phase			
H_2	27.775	1.83×10^{-2}	6.56×10^{-4}
O_2	13.877	8.27×10^{-39}	2.97×10^{-40}
Cl_2	2.50×10^{-3}	6.41×10^{-24}	2.30×10^{-25}
S_2	0	6.40×10^{-33}	2.30×10^{-34}
N_2	4.87×10^{-2}	4.87×10^{-2}	1.75×10^{-3}
H_2O	0	27.754	9.97×10^{-1}
HCl	0	5.00×10^{-3}	1.80×10^{-4}
H_2S	0	7.50×10^{-4}	2.70×10^{-5}
Solid Phase			
$CdCl_2$	0	0	
CdS	0	2.50×10^{-3}	
$CdSO_4$	0	0	
CdO	0	0	
Cd	2.50×10^{-3}	0	
S	3.25×10^{-3}	0	

Blank Page

REFERENCES

1. Ma, Y., and R. Bube, 1977: "Properties of Films Prepared by Spray Pyrolysis," J. Electrochem Soc., Vol. 124, No. 9, pp. 1430-1435.

2. Kasmerski, L.L., P.J. Ireland, F.R. White, and R.B. Cooper, 1978: "The Performance of Copper-Ternary Based Thin-Film Solar Cells," Proc. 13th IEEE Photovoltaic Specialists Conference, Washington, D.C. (5-8 June), pp. 184-189, Publ. 78CH1319-3 (Institute of Electrical and Electronic Engineers, New York, New York).

3. Marucchi, J., M. Petroin, Oudeacoumer, J. Bougnot, and M. Savelli, 1978: "Influence of Heat Treatment on Properties of CdS Sprayed Films," Proc. 13th IEEE Photovoltaic Specialists Conference, Washington, D.C. (5-8 June), pp. 298-302 Publ. 78CH1319-3 (Institute of Electrical and Electronic Engineers, New York, New York).

4. Smith, F.G., 1977: "Structures of Zinc Sulfide Materials," Am. Minerologist, Vol. 40, pp. 658-673.

5. Short, M.A., and E.G. Steward, 1957: "Effect of Grinding on the Structure of Zinc and Zinc-Cadmium Sulfides," Z. Physik. Chem., Vol. 13, pp. 298-315.

6. Palmberg, P.W., G.E. Riach, K.E. Weber, and N.C. MacDonald, 1972: Handbook of Auger Electron Spectroscopy (Physical Electronics Industries, Inc., Edina, Minnesota).

7. Buldhaupt, L.F., R.A. Mickelson, and W.S. Chen, 1980: "Cadmium Sulfide/Copper Ternary Heterojunction Cell Research," paper presented at CdS/Cu_2S and CdS/Cu-Ternary Photovoltaic Cells, SERI Subcontractors In-Depth Review Meeting, Washington, D.C. (3-5 September).

8. Loferski, J.J., et al., 1980: "Thin Film Cadmium Sulfide/Mixed Copper Ternary Heterojunction Solar Cells," Final Technical Progress Report, SERI Contract XL-9-8012-2 (March).

9. Nakayama, N., H. Matsumoto, K. Yamaguchi, S. Ikegami, and Y. Hiske, 1976: "Ceramic Thin Film CdTe Solar Cell," Jpn. J. Appl. Phys., Vol. 15, No. 11, pp. 2281-2282 (November).

10. Brodie, I., and J.B. Mooney, 1978: "Physical Processes in Charge Transfer Radiography," paper presented at annual meeting of IEEE Applications Society, Toronto, Canada (1-5 October).

11. Nakayama, N., H. Matsamo, A. Nakano, S. Ikegami, H. Uda, and T. Yamashita, 1980: "Screen Printed Thin Film CdS/CdTe Solar Cell," Jpn. J. Appl. Phys.,Vol. 19, No. 4, pp. 703-712 (April).

12. Zanio, K, and F. Krajenbrink, 1980: paper presented at SERI Emerging Materials Contractors In-Depth Review Meeting, Denver, Colorado (5-7 February).

13. McDonald, G., and G. Goodman, 1980: "Commercialization of a Thick Film Solar Cell," Quarterly Report, SERI Subcontract XS-0-3104-2 under Contract EG-77-C-04-4042, Globe Union, Inc., Milwaukee, Wisconsin (March).

14. Matsumoto, H., N. Nakayama, and S. Ikegami, 1980: "Preparation and Photovoltaic Properties of Screen Printed CdS/Cu_2S Solar Cells," Jpn. J. Appl. Phys., Vol. 19, No. 1, pp. 129-134 (January).

15. Feigelson, R.S., A. N'Diaye, and S-Y Lin, 1977: "II-III Solid Solution Films by Spray Pyrolysis," J. Appl. Phys., Vol. 48, No. 7, pp. 3162-3164.

16. Ikegami, S, 1979: private communication (talk presented at SERI).

17. Nakano, A., H. Matsumoto, N. Nakayama, and S. Ikegami, 1979: "Screen-Printable Electrode Material for CdS and Its Application to

Solar Cells," Paper IIIa-3, Digest Tech. Papers 1st Photovoltaic Sci. & Engr. Conf. in Japan, 1979, pp. 64-64.

18. Nakayama, N., H. Matsumoto, A. Nakano, and S. Ikegami, 1979: "Low Temperature Synthesis of CdTe and Its Application to Solar Cells," Paper IIIa-4, Digest Tech. Papers 1st Photovoltaic Sci. & Engr. Conf. in Japan, 1979.

19. Prince, M.B., 1979: Trip report for 22 October, U.S. Department of Energy.

20. Handbook of Chemistry and Physics, 56th Edition, 1975: R.C. Weast, ed. (CRC Press, Cleveland, Ohio).

21. Mooney, J.B., 1973: "Impregnated Porous Photoconductive Device and Method of Manufacture," U.S. Patent 3,745,504 (10 July).